1. INTRODUCTION

1.1 General Background

In the solar system Earth is the only planet where life in all its forms thrives freely. One of the major reasons for this is the presence of an indispensable liquid for life - water. Man uses water not only for drinking but also for hydropower, transportation, irrigation etc. Nepal is rich in water resources. To many observers harnessing the immense water resources wealth of Nepal is seen as the key to achieving rapid economic growth and development of Nepal (Thapa, 1995).

Nepal is a land-locked country. It forms a barrier between the Tibetan plateau and the Gangetic plain along the southern slope of the Himalaya. For about eight months (October to May) most of the rivers derive water from snow melt, spring and ground water recession. During this period the flow is in tranquil state. In the four months of the rainy season (June to September) all the rivers turn into a violent mass of water and sediment. Rainfall occurs due to the south-west monsoon. The humid monsoon air stream blowing from the Bay of Bengal is forced to rise as it meets the Himalaya. As a result heavy rainfall occurs on some sections of the southern Himalayan slopes. Rainfall is also high along the Churia range. In the leeward side of the ranges, rainfall is reduced due to rain shadow effect.

Based on the rainfall records collected by the Department of Hydrology and Meteorology (DHM) Nepal, in a year, receives about 1500 mm rainfall in a good monsoon regime (Dixit, 1995). More than 80% of the total annual rainfall occurs during the monsoon period (MFD).

In winter, rainfall is caused by the weather system originating in the Mediterranean region. The rains in their dying stages reach Nepal and cause significant precipitation in western where its influence tends to be stronger than in the east. The pre-monsoon months are characterized by thunder showers and squalls.

In the northern Himalayan region precipitation occurs in the form of snow. Glaciers and snow contribute significantly to the runoff of the major rivers of Nepal and dominantly influence the hydrological behavior. Accumulated snow acts as a reservoir which releases water after melting.

About 8% of the country's area is estimated to be under permanent snow cover (Dixit, 1995). The snowline is lowest in the March which gradually recedes with the advent of spring when melting of the accumulated snow begins.

The Himalayan Rivers originate in the snow-capped regions in the north. The flow of these rivers is derived from snow melt. The rivers carry significant flows in the dry season, and important for the purpose of drinking, irrigation and hydropower development. The flow of these rivers follows the rainfall pattern. Even though the rivers have significant dry season flow which is derived from groundwater recession, it is less compared to the runoff volume available during the monsoon.

The Mahabharata Rivers are rain-fed and get supplemented by the recharge from the spring, run-off and ground water recession. As a result, the hydrology of these rivers is characterized by low dry season flow and high flow during the monsoon period.

The Churia Rivers are rain-fed and have small drainage area so they are flashy with very low dry season flow.

All these large and small rivers give rise to about 6000 rivers totaling about 45,000 km in length. The drainage density of 0.3 km/km^2 of lateral drainage reflect the closeness of the drainage channels. Approximately 1000 of these rivers are more than 10 km long and about 100 of them are longer than 160 km (Dixit, 1995).

The hydrology of the basin is governed by the type of basin where rivers originate. There are different kinds of hydrological models that are used to study the hydrology of a basin. A model is a simplified representation of a complex system (Varshney, 1986). Hydrological models are models of hydrological systems. The hydrological models are used to estimate and predict water quantities and flow rates for a given scenario and assess the effectiveness of best water management practices. On the basis of process description, hydrological models can be classified into three groups:

a. Empirical Black-Box Models (Data-Driven Models)

These models are based on the relationship between input and output data and they do not take into account the physical process. The advantages of DDM are their simplicity, easy modeling approach and rapid computation time. The limitations are that they cannot extrapolate, and need adequate as well as reliable data, and cannot reflect any changes in the system. There are three types of empirical models which are as follows:

I. Empirically hydrological models, e.g. Unit hydrograph
II. Statistically based models, e.g. Linear regression, Correlation, AR, ARMA
III. Hydro-informatics based models, e.g. Neural network

b. Conceptual Models

They are based on simplified and conceptualized representation of the physics of the system. They represent catchment as a series of storage components and fluxes with semi-empirical type of equations. The model parameters cannot usually be assessed from field data alone, but have to be obtained through the help of calibration. Conceptual models are reliable in forecasting the most important features of the hydrograph. However, the implementation and calibration of such model can typically present various difficulties, and they cannot provide reliable result outside the range of calibration. The examples of conceptual models are NAM, HBV, Tank etc.

c. Physically Based Models

They are based on the physics of the system, i.e. the equations representing the processes are based on the principle of conservation of mass, momentum and energy. The differential equations, which represent the processes, are solved by numerical methods. The models parameters of such models are in principle measurable in the field. These models can in principle be applied to almost any kind of hydrological problem. They are applicable to ungauged basins and prediction of the effects of catchment change. However, these models require large amount of information, which is difficult to obtain and considerable expertise and computation time. For e.g. MIKE SHE

On the basis of spatial representation, hydrological models are divided into two types which are as follows:

I. Lumped Models: They represent catchment as a one unit. All parameters and variables represent average values over the entire catchment. Such model structures are most applicable to small areas in which the physical characteristics are relatively homogeneous
II. Distributed Models: They represent catchment as a combination of grids, sub-catchments or hydrologically similar units.

On the basis of aspect of randomness, hydrological models can be categorized into two types:

I. Deterministic Model: A deterministic model does not consider randomness; a given input always produces the same output. Such model expresses the domain (physics) of system by equations.
II. Stochastic Model: A stochastic model considers the randomness.

1.2 Need of the Study

The BTOPMC model can be applied to the large River basin for simulating the daily and hourly flow. The model can be successfully applied for hydrological simulations (flood forecasting, sedimentation, irrigation, water use etc.) in the large River basin. The model could achieve equal accuracy all over the basin i.e. at any sub basin. This fact is very important when modeling large catchments. However, it is noted that the calibrated parameter set depends on the spatial and temporal resolution of the model application. So it is necessary for finding relationships between calibrated parameter values and the physical catchment characteristics to enable the model to use without calibration which is extremely important in the case of applying the model to ungauged or data poor regions. Hence simulation of the daily flow of the Sunkoshi river basin is the need of this study.

1.3 Objectives of the Study

The hydrological modeling of the large river basin by using distributed hydrological models needs large amount of data. In the country like Nepal, most of the river basin is data poor or ungauged so use of global public domain datasets in the distributed hydrological model is the main objective of the study.

The specific objectives of the study are as follows:

1. To calibrate and validate the "Blockwise use of TOPMODEL with Muskingum-Cunge routing" method in the Sunkoshi river basin using the option "calculate using soil and land cover data" for Srmax calculation.
2. To calibrate and validate the "Blockwise use of TOPMODEL with Muskingum-Cunge routing" method in the Sunkoshi river basin using the option "calculate using soil and land cover data" for Srmax calculation.
3. To use the global public domain dataset for potential evapotranspiration calculations using Shuttleworth-Wallace (SW) model in BTOPMC.

1.4 Scope of the Work

According to the objectives, the scope of work includes application of Win BTOPMC, Arc View GIS 3.2/Arc Info, Google Earth, MS Excel, BTOPMC preprocessor tool and other BTOPMC tools. These techniques can provide effective and efficient means for hydrological modeling in large watersheds. This work includes satellite-based image of DEM (USGS), NDVI data (NOAA), soil data, land cover data, mean daily temperature, diurnal temperature range, actual vapor pressure, cloud cover, wind speed, extraterrestrial radiation and possible duration of sunshine data to predict the flow. Most of the data which are freely available in public domain were used. Therefore, it could be the better option to use as a runoff simulating tool because Nepal has many ungauged basins. The BTOPMC model uses the Shuttleworth-Wallace model to calculate the potential evapotranspiration (PET). To calculate this, the publically available datasets are used. The PET is a major input to run the BTOPMC and other distributed models.

1.5 Limitations of the Study

The followings are the limitations of the study:

- Meteorological element such as air temperature was not found in the Himalayan region of the basin.
- Due to lack of advance techniques, equipments and accountability on data collection, the stream flow data and meteorological data analysis do not show consistency.
- Lack of sufficient amount of temperature and precipitation data.
- About 27 % of the basin lies in Tibet, China. Therefore, the rainfall and temperature data from that part of basin were not taken for this study.

2. REVIEW OF LITERATURE

The review of literature is concerned with receiving some knowledge, information ideas relevant to the topic of the study. Every study is based on the past study. The past knowledge or the previous studies should not be ignored as it provides foundation to the present study.

The purpose of reviewing the literature is to develop some expertise in one's area to see what new contributions can be made and to receive some ideas for developing a research design (Howard K. Wolf and Prem Raj Pant, 2003:34)

This chapter deals with review of books, reports, research papers, and unpublished publications related to hydrological modeling.

2.1 Hydrological Modeling System

The hydrological modeling system simulates the precipitation-runoff process of a watershed system. It is designed to be applicable in a wide range of geographic areas for solving the widest possible range of problems. Hydrographs produced by the models are used for studies of water availability, urban drainage, flood forecasting, future urbanization impact, reservoir spillway design, flood damage reduction, flood plain regulation and systems operation.

Hydrological models are divided into two categories. They are physical models and analog models. Physical model represent the system on a reduced scale, e.g. a hydraulic model of a dam spillway. Analog model uses the physical system having properties similar to the prototype.

Abstract model represent the system in mathematical form. The system operation is described by a set of equations linking input and output variables. These variables are the functions of space and time may also be probabilistic or random variable that does not have fixed value at a particular space and time.

The deterministic model does not consider randomness, i.e. a given input always has the same output. The stochastic model has output that are at least partially random. If random variation is large, the stochastic model is more appropriate. The deterministic model is further classified as

lumped and distributed model on the basis of spatial variation. In the lumped model, the system is spatially averaged or regarded as a single point in space without dimension. The distributed model considers the different hydrological processes at various points in space and defines model variables as function of space dimension. On the other hand, the stochastic model is classified as space independent and space correlated whether or not the random variables influence each other. On the basis of temporal variation, the distributed model is classified as steady and unsteady flow whereas the stochastic model is classified as time independent and time correlated.

2.2 Distributed Hydrological Model

Distributed hydrologic models feature the capability to incorporate a variety of spatially varying data from a proliferating set of databases on land use, land and soil characteristics, and high resolution precipitation, temperature, and other forcing unit. In addition to facilitating simulations and predictions with higher resolution than lumped models, this feature offers the potential to improve hydrologic predictions on current operational scales by accounting for the inherent spatial variability that has historically been lumped into average watershed characteristics (Smith et al., 2004).

Some of the desirable characteristics of distributed hydrological model are as follows:

1) Accurate water balance accounts

   As the hydrological memory is long in a large basin, a long term water balance is critical and no significant estimation error should be allowed. The water balance is governed by the equation:

   S = P-E-Q

   Where,

   S = Storage

   P = Precipitation

E = Evapotranspiration

Q = Other Losses

2) Equal simulation accuracy over the entire basin

In a large basin, it is important to have equal simulation accuracy all over the basin. As the vertical processes in each grid cell are independent in distributed hydrological models, the overall accuracy is controlled by the accuracy of each cell.

3) All primary hydrological processes considered

As many different climatic and geographical regions may be included in a large basin, the model should consider all the primary hydrological processes present in the basin. They should include precipitation, radiation, evapotranspiration, snowmelt, interception, infiltration, surface runoff, surface soil moisture, unsaturated zone storage, groundwater recharge and discharge. Sediment and nutrient production and transport should also be included. Each component's accuracy controls the aggregate model performance.

4) Flexible selection of unit time and space intervals

The model should work in different time and space intervals responding to various data availability, user requirements, computer capacity etc. The narrowest portion of a basin also controls the choice of spatial interval.

5) Parsimonious parameter set

As any large basins include information of poor or ungauged sub-basins, regardless of the size of the basin and the number of grid cells in the basin, the model parameters to be identified should not increase. The resolution of land cover information necessary to identify the parameters should be within the available precision.

6) Link with satellite and GIS data

   For the same reason mentioned in (5), satellite information and various global and local data sets are necessarily used in simulating large basins. The model should therefore be equipped with the ability to link with the global data sets.

7) User friendly interface

   As demand of large basin simulation often exists in developing countries with serious lack of data, the model should be accessible and usable by professionals of any part of the world preferably with proper capacity building programs.

8) Incorporation of water use system:

   Any large basin is extensively disturbed by human activities. The water use system such as water storage, detention, flow control, withdrawal, diversion, transfer, distribution, use, consumption, return flow, treatment, recharge etc. should be incorporated in the model. Irrigation, municipal and industrial water uses and reservoir controls are especially important as they totally alter the water balance and hydrographs of a basin.

2.3 Different Types of Hydrological Modeling Systems

There are many hydrological modeling systems available. Some of them are discussed briefly below:

2.3.1 HEC-HMS

HEC-HMS (Hydraulic Engineering Center Hydrologic Modeling System) was developed for the U.S. Army Corps of Engineers. It is specifically designed for simulation of rainfall-runoff processes of networking watershed systems. Modeling components includes losses, runoff transform, open-channel routing, and analysis of meteorological data, rainfall-runoff simulation, and parameter estimation and reservoir simulations. The physical representation of watersheds or basins and rivers is configured in the model based on representation of general hydrologic elements, including sub-basins, reaches, junctions, reservoirs, diversions, sources, and sinks. The system encompasses

losses, runoff transform, open-channel routing, analysis of meteorological data, rainfall-runoff simulation, and parameter estimation. A wide array of options is available to simulate losses, including initial and constant rates, the SCS curve number method, and the Green-Ampt method. Runoff transform methods include the Clark, Snyder, and SCS unit hydrograph techniques. User-specified unit hydrograph ordinates can also be used. Open-channel routing methods include the lag method, Muskingum method, the modified Puls method, the kinematic wave method, and the Muskingum-Cunge method. Meteorological data analysis can also be performed in the model for precipitation and evapotranspiration and includes various historical and synthetic methods (HEC, 2001). The model suffers from the following limitations:

- Cannot simulate water quality processes
- Relatively difficult to use in conjunction with other water quality models
- Cannot simulate groundwater levels

2.3.2 TANK Model

In 1961 Sugawara developed tank model which was a continuous, lumped model. Tank model is a series of storage type model to account for the nonlinear relationship between the rainfall and runoff. The storage type model is based on the hypothesis that runoff and infiltration are functions of the amount of water stored in the ground. Several components of discharge such as surface, subsurface and base flows are represented in the model.

The tank model is a simple model composed of several tanks arranged vertically in series. Rainwater is fed into the top tank. Water in each tank partially discharges through the side outlet and partially infiltrates through a bottom outlet to the next lower tank. River discharge can be simulated as the sum of the outputs from the side outlet of each tank. This model is effective if we have long records of observational data for calibration and validation. Though this model was found to be effective, it cannot be used to simulate the response of the catchment to the variations occurring in the catchment as It cannot determine parameters related to soil, vegetation etc. to which the response of catchment is most sensitive.

2.3.3 Xinanjiang Model (XJM)

The Xinanjiang model (XJM) was developed by Zhao and others in 1980. This is a conceptual model with distributed parameters corresponding to the various sub catchments. The concept of runoff formulation is introduced to estimate effective rainfall. The DRH is computed by the lag and route model and then routed through channels by the Muskingum method. The model has nine somewhat insensitive parameters computed from observed hydrological data, and the remaining four parameters need to be estimated carefully. The XJM has been widely used in humid and semi arid areas of the People's Republic of China.

2.3.4 SCS-CN Method

The SCS-CN method of estimating runoff volumes from rainfall is simple and easy to use. The curve number method was developed by the USDA Natural Resources Conservation Service, which was formerly called the Soil Conservation Service or SCS. It was developed from a great deal of unpublished data. It works well for a wide range of agricultural soil cover complexes. It is widely used in a wide range of design conditions by the practicing engineers and hydrologists. The CN (curve number) is an empirical parameter used in hydrology for predicting direct runoff or infiltration from rainfall excess. It is widely used and is an efficient method for determining the approximate amount of direct runoff from a rainfall event in a particular area. There appears to be no regional variation in CN for the same cover type. However, the lack of data may be influencing this conclusion but there appears to be seasonal variation in certain forested CN.

2.3.5 MIKE-SHE

MIKE SHE is an advanced integrated hydrological modeling system. It simulates water flow in the entire land based phase of the hydrological cycle from rainfall to river flow, via various flow processes such as, overland flow, infiltration into soils, evapotranspiration from vegetation, and groundwater flow.

MIKE SHE has been applied in a large number of studies world-wide focusing on e.g. conjunctive use of surface water and ground water for domestic and industrial consumption and irrigation, dynamics in wetlands, and water quality studies in connection with point and non-point pollution.

It is used in regional studies covering entire river basins as well as in local studies focusing on specific problems on small scale.

2.3.6 About TOPMODEL

TOPMODEL is based on source area concept of hill-slope hydrology, which has been applied to basins of few hundred km^2. As the model considers catchment as an aggregate of heterogeneous land areas, it is practically impossible to calibrate model parameters for large basins. Therefore, BTOPMC model has been developed in order to apply the concepts of TOPMODEL ranging from smaller to large basins.

The main features of TOPMODEL are as follows:

1. The whole basin is considered as a collection of many hill slopes. The hill slope is the unit of water balance and there is no water exchange between hill slopes.
2. In steady state (after the holding capacity has been filled), the effective rainfall over a hill slope discharges either as overland flow from the fractional area that is saturated or as sub-surface flow from the outlet of the hill slope, or both.
3. The hydraulic gradient is assumed parallel to the land surface.
4. In the steady state, sub-surface flow from the outlet of the hill slope is equal to recharge rate over the hill slope (assumed homogeneous) times the area of hill slope (Continuity equation).

   $$q_{bi} = f(a_i / dl_i) r_i \qquad (2.1)$$

   Where

   q_{bi} = sub-surface flow from the hill slope per unit contour length ,

   a_i = area of the hill slope per unit contour length and

   r_i= recharge rate
5. The groundwater discharge from the hill slope outlet is related to the saturation deficit (Momentum equation)

   $$q_{bi} = T_0 \exp(-SD_i / m) \tan\beta_i \qquad (2.2)$$

T_0 = Lateral transmissivity of the hillslope,

SD_i = saturation deficit in the unsaturated zone,

m= discharge decay factor,

$\tan\beta$ = outlet slope.

Using equations 2.1 and 2.2, the local saturation deficit (SDi) is derived as

$$SD_i = \overline{SD} + m(\lambda - \lambda_i) \qquad (2.3)$$

where $\overline{SD}$ = average saturation deficit, λ_i = topographic index and λ = catchment average topographic index.

6. The topographic index is represented by the following equation:

$$\lambda = \ln\left[(a_i / dl_i)/T_o \tan\beta_i\right] \qquad (2.4)$$

The topographic index is a very important concept in TOPMODEL; it represents the tendency of any point in the catchment to develop saturated conditions. In particular, it reflects the tendency of water to accumulate and store at any point in the catchment (in terms of a_i and T_0) and the tendency for gravitational forces to move that water down slope (expressed in terms of $\tan\beta_i$ as an approximate hydraulic gradient). A high index implies that it is easier for the soil profile to be saturated and lead overland flow.

2.4 Review of Related Previous Studies

Aryal, Sagar (2007) in his study "**Application of a Distributed Hydrological Model – BTOPMC in Narayani River Basin**" presented that the model has good performance for main outlet as well as other sub basin outlet. At the main basin outlet, Narayanghat, the Nash Sutcliffe coefficient was 88.62% in calibration. The simulated peak flow for Narayani river basin main outlet is the best among all other sub-basins. The Nash-Sutcliffe coefficient was 88.03% in validation. Therefore he concluded that the BTOPMC model is applicable and reliable model for carrying out research in large river basins.

Baral, Sanjeeb (2007) in his study "**Applicability of Semi-distributed Hydrological Model (BTOPMC) in Bagmati River Basin**" has applied BTOPMC model to the Bagmati river basin for simulating the daily flow. His study indicated that the model can be used successfully for the hydrological simulation of the Bagmati river basin.

The Nash efficiencies of 79.77% and 76.24% and volume error or 10.24% and 24.05% were obtained for the calibration and validation of the model respectively using 1 km resolution DEM. Similarly, the Nash efficiencies of 73.06% and 73.62% and volume error of -0.29% and 18.44% were obtained from the study of impact of grid resolution of DEM for the year 1999-2000 and 1997-1998 respectively using 250 m resolution DEM. And, he recommended the use of BTOPMC model with the use of globally available public domain data as input for the integrated water resources planning and management in the context of the data-poor large basins of Nepal.

He also compared the monthly average PET from Shuttleworth-Wallace Model as global data input and FAO Penman's method as local data input and found to be in acceptable accuracy.

Takeuchi, Kuniyoshi et al. (1999), in his research paper "**Introduction of block-wise use of TOPMODEL and Muskingum-Cunge method for the hydro-environmental simulation of a large ungauged basin**", has proposed BTOPMC model for use as a hydro-environmental simulation model. Hydro-environmental simulation is essential for the sustainable management of water resources. There are many large ungauged basins in the world which need integrated planning for development and management and where the lack of data is a serious barrier for any application of a basin-wide hydro-environmental simulation model. To overcome such a barrier, the use of satellite observations can play an important role. For this purpose a method is required that can make use of remotely sensed data. A hydrological simulation model, the block-wise use of TOPMODEL and the Muskingum-Cunge flow routing, was used as a promising model in this direction.

He presented two examples to demonstrate the potential use of the new model: one for the 3570 km^2 Fuji-Kawa basin, Central Honshu, Japan and the other for the 20,750 km^2 northern part of Minjiang basin, an upper branch of Changjiang (the Yangtze river), China. The Fuji-Kawa is the case where ample hydrological, land-use and geological data are available while the Minjiang case

demonstrates the application to a river basin where only geographical elevation data and some precipitation data are available.

Hapuarachchi et al. (2008) in his research "**Investigation of the Mekong River Basin Hydrology for 1980-2000 using the YHyM**", has investigated the hydrological behavior of the Mekong River Basin using a distributed (grid based) hydrological model, YHyM during the period 1980-2000. Overall performance of the model was found to be good and the detailed analysis on the seasonal variation of soil moisture, actual evapotranspiration, interception evaporation, and runoff estimations indicate that the YHyM could replicate the natural hydrological responses of the basin well. In addition, the model accuracy (discharge and potential evaporation) at some selected internal points of the basin is also good signifying that the YHyM can achieve equal accuracy at each point in the basin which is very important in water resources management, planning, and decision making. However, other applications of YHyM show that its performance in arid regions is relatively poorer compared to humid regions due to the extremely complex hydrological processes which are difficult to understand.

Shrestha et al. (2007), in their research paper "**The Assessment of Spatial and Temporal Transferability of a Physically Based Distributed Hydrological Model Parameters in Different Physiographic Regions of Nepal**", have tested the BTOPMC model for spatial and temporal transferability of the calibrated model parameters to predict various runoff components (runoff volumes, peak flows, and base flows) in different physiographic regions of Nepal.

The model was calibrated and validated in six river catchments located in the Siwalik and the middle mountain regions. Those catchment were Babai, Bagmati, East Rapti, Kamala, Kankai, and West Rapti. Then the model performance was evaluated in ungauged catchments Manahari and Tinau with parameters spatially transferred from gauged catchments and found good. Two scenarios (scenario A and scenario B) were tested to evaluate the temporal transferability of calibrated model parameter in the Bagmati river catchment. In both scenarios only marginal deviation of model performance from the calibrated model was observed. The study suggested that the calibrated parameters of BTOPMC model can be spatially and temporally transferred between and within river

catchments located in similar physiographic regions to simulate runoff in response to minor land use and climate change scenarios.

Dulal et al. (2006) in their research paper, "**Evaluation of a physically based distributed hydrological model, BTOPMC, for different physiographic zone of Nepal**" have evaluated the performance of the distributed hydrological model, BTOPMC for different physiographic zones of Nepal and then developed a regional model which can be used for prediction in ungauged basins. The BTOPMC model was calibrated and validated for six basins. The result showed that the model performs reasonably well for most of the basins. Then a simple regional model was developed for evaluating the regional model. The parameters of the regional model were applied to the seventh basin which was not used for developing the regional model. The result showed that the parameters derived for the regional model give satisfactory performance. Therefore he concluded that BTOPMC can be used for prediction in ungauged basins in Nepal.

Ishidaira et al. (2006) in their research paper "**Relating to BTOPMC Model Parameters to Physical Features of MOPEX Basins**" have investigated the possibility of establishing an improved physically based a priori parameter estimation technique, based on relating hydrological model parameters to physical basin features using the distributed hydrological model BTOPMC. They observed that the results of the 39-year 'blind' a priori estimations for the ten basins quantitatively showed that the model parameters cannon be reasonably and confidently estimated without the use of parameter transfer functions. The results of the 20 year calibrations using the SCE-UA method and the 19-year validations indicated that BTOPMC's predictive accuracy is strongly dependent on calibration accuracy, implying well optimized parameter values should ensure model predictive accuracy. Thus it is suggested to use well-calibrated parameter values to make parameter transfer function.

Hapuarachchi et al. (2007) in their research paper "**Importance of Rainfall Measurements for the Flood Forecasting of the Mekong River Basin**" have presented the results of an application of a grid based distributed hydrological model, BTOPMC to the Mekong river basin and the overall performance was found to be good. However, it is observed that the accuracy of model results (with gauged precipitation data) is significantly diminished due to lack of gauged precipitation data. Basically most of the peak flow events are over estimated though the low flow events are well

simulated. Therefore, it is suggested to establish well maintained adequate number of rain gauges in the Mekong river basin. Detail analysis on the seasonal variation of soil moisture, evapotranspiration, interception and runoff estimations indicate that BTOPMC could replicate the natural hydrological response of the basin well.

Hapuarachchi et al. (2005) in their paper " **Hydrological modeling and flood simulation of the Fuji River basin in Japan**" applied the BTOPMC model to the Fuji River basin for simulating the daily and hourly flow. Result indicated that the model can be successfully applied for hydrological simulations (flood forecasting, accounting sedimentation, water use etc) in the Fuji River basin and could achieve equal accuracy all over the basin. It is also noted that the calibrated parameter set depends on the temporal resolution of the model application. It is suggested to find relationships between calibrated parameter values and the physical catchment characteristics to enable the model to use without calibration which is extremely important in the case of applying the model to ungauged or data poor regions.

2.5 Summary

There are many river basin simulation models. Each has different temporal and spatial characteristics and data requirements. Thus selection of the most appropriate model for a given purpose and conditions is an important decision. Following a review of a number of different models that could be adopted for use as simulation models, it is revealed that a model applicable to a large ungauged basin is still missing. In many countries, including Nepal, there are large ungauged catchments awaiting development and management that would benefit from the use of hydrological simulation models to assist with basin planning. The selection of hydrological simulation models should consider a number of practical constraints present in such basins:

a) Precipitation, runoff, evaporation, and other hydro-climatological data are seldom available.
b) Land-use, geology, vegetation, soil-type and other basin characteristics data are also seldom available.
c) Extensive anthropogenic disturbances such as deforestation, urbanization and other basin developments are present.

Meanwhile electronically transmittable data become available to increasingly more users. Also large amounts of satellite and remote-sensing data are available at various wavelengths. These conditions prescribe the basic properties that a model has to have namely:

a. Digital elevation maps (DEMs) are used replacing a conventional stream network and topography map;
b. Satellite data can be utilized to identify land surface characteristics of the basin such as interception, soil types, infiltration capacity, evapotranspiration etc; and
c. Satellite and other remote-sensing data can be utilized for spatially-distributed and temporally continuous precipitation measurement.

In addition to these data-oriented criteria, the model should satisfy users requirements such as:

1. Simulation of floods and low flows at arbitrary points in a basin at an arbitrary time.
2. Simulation of large basins
3. Incorporation of effects of water resource systems such as dams, canals, paddy fields, irrigation network, municipal water distribution and use etc in the model and simulation.
4. Simulation of land-use changes as well as climatological variation.

Among many runoff simulation models currently available, none was found to satisfy all those conditions. There are several types of model such as Sugawara's Tank, SCS Curve Numbers, HEC-HMS, Xinanjiang, Nash model, etc. Their inability to explicitly handle land-use changes and water use systems modification make them unsuitable, without extensive modification, for the present requirements. More suitable types of model include distributed models (such as MIKESHE), but they are data demanding and not yet practical for large ungauged basins. Since there was no model that met the required specification, TOPMODEL was selected as a basis for developing a new model to meet the required needs. TOPMODEL is a combination of lumped and distributed modeling concepts which better qualifies to meet the conditions described above but it has generally been applied only to small basins. Therefore to extend its use to large basins, BTOPMC has been introduced. The BTOPMC, which is still under development, is able to meet most of the user requirements using the kinds of data generally available. It has two distinct advantages when applied to ungauged basins. They are as follows:

- It has the advantages of both a lumped model and a distributed model.
- The model is heavily dependent on a soil-topographic index that can be identified through digital elevation model (DEM) and satellite information without extensive ground observations (Takeuchi, 1999).

3. DESCRIPTION OF MODEL

The BTOPMC refers to "Blockwise use of TOPMODEL with Muskingum-Cunge routing". This model was developed at the University of Yamanashi, Japan. BTOPMC implements the concepts of TOPMODEL with Muskingum-Cunge method for flow routing. The model performs distributed calculations of flows, but it is conceptually semi-distributed in terms of parameterizations. TOPMODEL is based on source area concept of hillslope hydrology, which has been applied to basins of few hundred km^2. As the model considers catchment as an aggregate of heterogeneous land areas, it is practically impossible to calibrate model parameters for large basins. Therefore, BTOPMC model has been developed in order to apply the concepts of TOPMODEL ranging from smaller to large basins. The fig 3.1 shows the history of development of BTOPMC model.

Fig 3.1

History of Development of BTOPMC

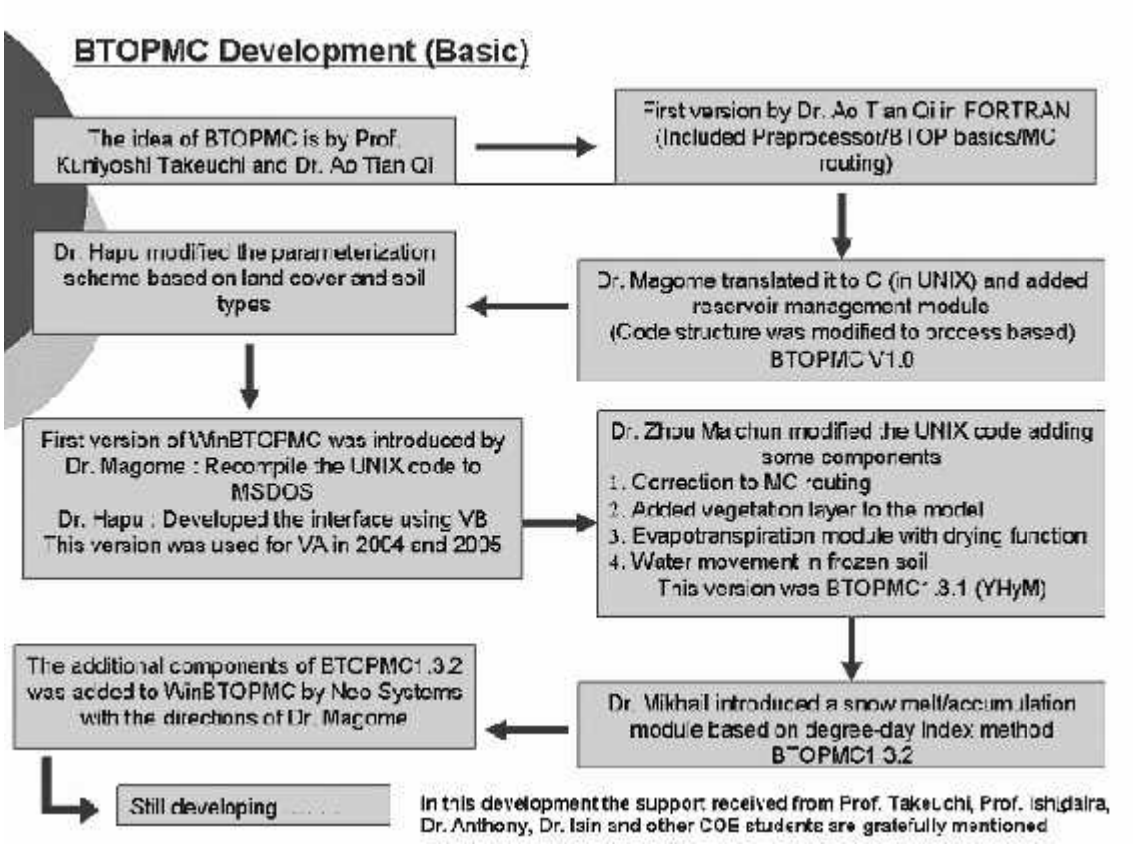

Source: CREEW

3.1 Main Features

The main features of BTOPMC model are as follows:

- The basin may be divided into a number of blocks (or sub-basins) each of which may consist of several hillslopes and sub-surface water is assumed to be shared within each hillslope, but not between blocks.
- In steady state (after the holding capacity has been filled), the effective rainfall over a block discharges either as overland flow from each grid cell that is saturated, or as sub-surface flow to a local stream segment schemed in each grid cell in the block, or both.
- In steady state, sub-surface flow from each grid cell is equal to the recharge rate in a block (assumed homogeneous over a block) times the effective contributing area of the grid cell i (Continuity equation).

$$q_{bi} = a_i f(a_i) r_k / a_{0i} \qquad (3.1)$$

where q_{bi} = specific base flow of the grid cell i to the local stream segment per unit grid cell, $a_i.f(a_i)$ = effective contributing area, r_k = recharge rate, a_{0i} = area of the grid cell i. The effective contributing area ratio, $f(a_i)$ is the ratio of the net upstream catchment area that contributes to the discharge from the grid cell i to the total upstream area a_i.

The function $f(a_i)$ is taken to be equal to one in BTOPMC (from V1.0 to V1.3.2).

- The discharge generated at the grid cell outlet is expressed in terms of the saturation deficit of the outlet grid cell in the form (Momentum Equation)

$$q_{bi} = T_0 \exp(-SD_i / m) \tan\beta_i \qquad (3.2)$$

where T_0 = Saturated transmissivity for grid cell i, m = block average decay factor, SD_i = local saturation deficit and $\tan\beta_i$ = slope of the grid cell.

- Discharge generated at each grid cell flows into a local stream segment for that cell. Stream-flow is then routed via an open channel from any upstream origin to the basin outlet.
- The Topographic index in the BTOPMC model is given by

$$\lambda_i = \ln \frac{a_i f(a_i)}{\tan\beta_i} \qquad (3.3)$$

3.2 Saturation Deficit

The storage deficit at the grid cell is calculated as the average one of the sub-basin plus a deviation because of the difference between the soil-topographic indices at the grid and over the sub-basin:

$$SD(t) = \overline{SD}(t) + m(\lambda - \ln[a/(T_0 \tan\beta)]) \quad (3.4)$$

where λ is the sub-basin average of the soil-topographic index, $\ln[a/(T_0 \tan\beta)]$, and the sub-basin average of storage deficit is obtained from a time step ahead storage deficit, groundwater recharge and release of the sub-basin as:

$$\overline{SD}(t+1) = \overline{SD}(t) + \overline{q_v}(t) - \overline{q_b}(t) \quad (3.5)$$

Where, $\overline{q_v}(t)$ and $\overline{q_b}(t)$ are averaged values of recharge and base flow in the sub-basin (mm day^{-1}).

3.3 Hydrological Processes for a Grid Cell

Fig 3.2

Vertical Soil Profile in a Grid Cell

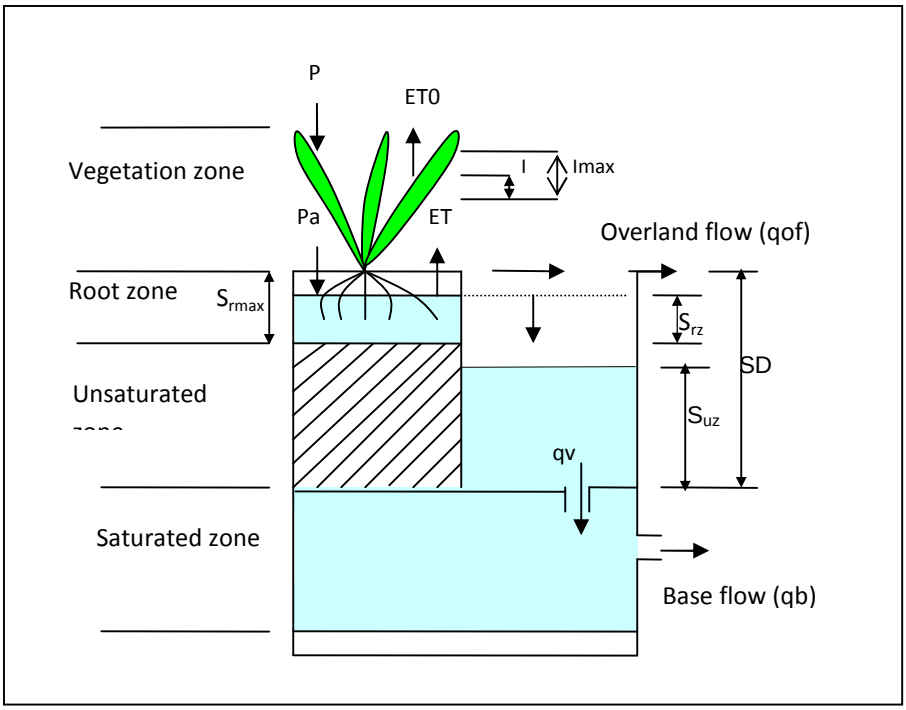

Source : Dulal, 2008

Land surface is covered by vegetation canopy. The vertical soil profile is divided into three layers:

- Root zone
- Unsaturated zone (inactive part contains static moisture content whereas in active part, moisture content varies with time)
- Saturated zone

Raindrops falling on vegetation canopy will be first intercepted by leaves up to the interception capacity. The intercepted water undergoes evaporation; the net rainfall reaches to the land surface and fills the root zone. The evapotranspiration is considered to occur from the root zone according to the potential evapotranspiration and the availability of water in the root zone. When the root zone storage reaches its maximum capacity, the excess water infiltrates into the unsaturated zone. The saturated zone receives flow from the unsaturated zone. The outflow from the saturated zone constitutes base flow. If the storage in the unsaturated zone exceeds the saturation deficit, then the excess becomes overland flow. The discharge in each cell is composed of both overland flow and base flow.

Equations

I. Interception evaporation in Vegetation zone

The interception storage capacity, I_{max},is given by

$$I_{\max} = C_{\text{int}} LAI \qquad (3.6)$$

where C_{int} is the interception coefficient. (C_{int} = 0.2 is used).

The interception deficit, $D_{int}(t)$, is given by

$$D_{\text{int}}(t) = I_{\max} - I(t-1) \qquad (3.7)$$

Interception evaporation, $ET_o(t)$, is calculated as

$$ET_o(t) = \begin{cases} \min[I_{\max}, PET_o(t)] & P(t) > D_{\text{int}}(t) \\ \min[I(t-1) + P(t), PET_o(t)] & P(t) \le D_{\text{int}}(t) \end{cases} \qquad (3.8)$$

where $D_{int}(t)$ is the interception deficit (mm), I(t-1) is storage state of interception at previous time step (mm), $ET_o(t)$ is the interception evaporation (mm day^{-1}), $PET_o(t)$ is the potential evaporation for the interception (mm day^{-1}), P(t) is the gross rainfall above the canopy (mm day^{-1}).

Updated interception, I(t), is given by

$$I(t) = \begin{cases} I_{\max} - ET_o(t) & P(t) \geq D_{\text{int}}(t) \\ I(t-1) + P(t) - ET_o(t) & P(t) < D_{\text{int}}(t) \end{cases} \quad (3.9)$$

Net rainfall on the land surface, $P_a(t)$ is given by

$$P_a(t) = \begin{cases} 0 & P(t) < D_{\text{int}}(t) \\ P(t) - D_{\text{int}}(t) & P(t) \geq D_{\text{int}}(t) \end{cases} \quad (3.10)$$

II. Soil moisture in root zone and evaporation

The soil moisture deficit in root zone, $D_{rz}(t)$,,is calculated as

$$D_{rz}(t) = S_{r\max} - S_{rz}(t-1) \quad (3.11)$$

The soil moisture change in root zone, ζS_{rz} , is given by

$$\zeta S_{rz}(t) = \begin{cases} P_a(t) & p_a(t) \geq D_{rz}(t) \\ D_{rz}(t) & p_a(t) < D_{rz}(t) \end{cases} \quad (3.12)$$

$$S_{rz}(t) = S_{rz}(t-1) + \zeta S_{rz}(t) \quad (3.13)$$

Actual evapotranspiration from root zone, ET, is calculated as

$$ET = \min\{S_{rz}(t), G_{rz} PET(t)\} \quad (3.14)$$

where Grz is soil drying function, which is given by

$$G_{rz} = \begin{cases} \dfrac{1}{1 + \exp\{-\sim \cdot S_{rz}(t) / S_{r\max}\}} & S_{rz}(t) < S_{r\max} \\ 1, & S_{rz}(t) \geq S_{r\max} \end{cases} \quad (3.15)$$

Storage excess in root zone, q_{rz}, is calculated as

$$q_{rz} = \max\left(S_{rz}(t-1) + \zeta S_{rz}(t) - ET(t) - S_{r\max}, 0 \right) \quad (3.16)$$

Updated storage in the root zone is given by

$$S_{rz}(t) = S_{rz}(t-1) + \zeta S_{rz}(t) - ET(t) - q_{rz}(t) \quad (3.17)$$

III. Storage in Unsaturated zone

Storage in unsaturated zone, $S_{uz}(t)$, is given by

$$S_{uz}(t) = \begin{cases} S_{uz}(t-1) & q_{rz}(t) \leq 0 \\ S_{uz}(t-1) + q_{rz}(t) & q_{rz}(t) > 0 \end{cases} \quad (3.18)$$

IV. Groundwater recharge

The groundwater recharge, $q_v(t)$, is given by

$$q_v(t) = \min\left(K_0 \exp\left(-SD(t)/m\right), S_{uz}(t) \right) \quad (3.19)$$

The water storage in the unsaturated zone is updated after the infiltration to the saturation zone occurred as:

$$S_{uz}(t) = S_{uz}(t) - q_v(t) \quad (3.20)$$

V. Base flow

The base flow, $q_b(t)$, is given by

$$q_b(t) = T_0 \exp\left(-SD(t)/m'\right) \tan \beta_i \quad (3.21)$$

VI. Overland flow

The overland, $q_{of}(t)$, is given by

$$q_{of}(t) = S_{uz}(t) - SD(t) \quad \textit{subject to} \quad q_{of}(t) \geq 0 \quad (3.22)$$

The storage state is updated again as follows:

$$S_{uz}(t) = S_{uz}(t) - q_{of}(t) \quad (3.23)$$

VII. Total flow

Total flow is the sum of overland flow and base flow.

3.4 Flow Routing: Muskingum-Cunge Method

The Muskingum-Cunge method (Fig. 3) is useful for simulating a large stream network since it can successively calculate the flow rates at all stream-network nodes at a single time without being disturbed by the time differences of flow wave arrivals at each junction of streams. However, it cannot allow for backwater effects.

Fig 3.3

Muskingum-Cunge Method

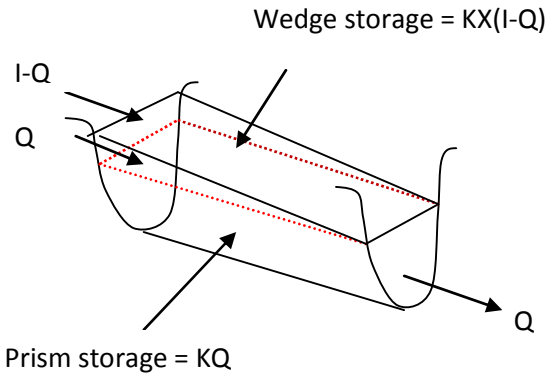

Continuity equation is given by

$$I_{t+\Delta t} - O_{t+\Delta t} = \frac{dS}{dt} \qquad (3.24)$$

where *I* is inflow, *O* is outflow and *S* is storage.

The storage equation is given by

$$S = KO + KX(I - O) \qquad (3.25)$$

where *K* is a proportionality coefficient and *X* is a weighting factor.

Solving continuity and storage equation, the equation relating to inflow and outflow is given as

$$O_{t+1} = C_1 I_{t+1} + C_2 I_t + C_3 O_t \quad (3.26)$$

where *C1*, *C2* and *C3* are constants (functions of parameters K and X).

$$C_1 = \frac{\Delta t - 2KX}{2K(1-X) + \Delta t} \quad (3.27)$$

$$C_2 = \frac{\Delta t + 2KX}{2K(1-X) + \Delta t} \quad (3.28)$$

$$C_3 = \frac{2K(1-X) - \Delta t}{2K(1-X) + \Delta t} \quad (3.29)$$

$$C_1 + C_2 + C_3 = 1 \quad (3.30)$$

In the Muskingum method, parameters *K* and *X* can be calibrated from observed inflow and outflow hydrographs by various methods such as trial-and-error. The variables *K* and *X* are handled as constants, with consideration of neither the physical characteristics of watercourses nor the temporal and spatial distribution of discharges.

The Muskingum-Cunge (M-C) method is a modified version of the Muskingum method. Cunge (1969) demonstrated that above Equation is equivalent to the finite-difference representation of the classic kinematic wave equation and the convection-diffusion model which accounts for wave attenuation but not for backwater effects. The routing parameters *K* and *X* in equations are computed as follows:

$$K = \frac{\Delta L}{c} \quad (3.31)$$

$$X = 0.5\left(1 - \frac{Q}{c B S_0 L}\right) = 0.5\left(1 - \frac{L_c}{\Delta L}\right) \quad (3.32)$$

where *K* is a storage constant having dimensions of time, and *X* is a weighting factor expressing the relative importance inflow and outflow have on the storage; *L* is the length of routing reach ; c and B are the kinematic wave celerity and diffusion coefficient of the kinematic wave equation, respectively; and $L_c = c/B$ is the characteristic length of the routing reach. c and B are determined from Manning's equation. *K* and *X* in M-C method are not constants in stream networks, but are distributed temporarily and spatially.

Expressions for μ, « and *h*

$$\mu = \frac{5}{3} q^{2/5} i^{3/10} n^{3/5} \quad (3.33)$$

$$« = \frac{h^{5/3}}{2n\sqrt{i}} \quad (3.34)$$

$$h = \frac{(nq)^{3/5}}{i^{3/10}} \quad (3.35)$$

where q = discharge per unit width (reference discharge), i = stream bed slope, n = Manning roughness coefficient and h = water depth

Final expressions for *K* and *X*

$$K = \frac{0.6 n^{0.6} \zeta L}{q^{0.4} i^{0.3}} \quad (3.36)$$

$$X = 0.5 - \frac{0.3(nq)^{0.6}}{i^{1/3} \zeta L} \quad (3.37)$$

3.5 Parameters of BTOPMC core model

The followings are the parameters of the BTOPMC model:

I. Decay factor of transmissivity (m)

m describes how the actual transmissivity decreases when the soil is not saturated. Although 'm' is a property impacting soil processes, its value is influenced by other factors in addition to soil type – land use in particular. For simplicity, therefore, BTOPMC considers m to be constant within a given block/ sub-basin and needs to be calibrated.

II. Roughness factor for a block (n_0)

n_0 is a scaling parameter to compute Manning's roughness for routing. Manning's roughness parameter (n) is used to represent the impact of stream channel roughness. It varies spatially and temporally. As it is not feasible to calibrate n for every stream channel element, BTOPMC uses a simple methodology to incorporate

spatial variability in n considering the impact of topography as a dominant factor, i.e. steeper slopes will have a higher resistance to flow than shallower slopes.

In BTOPMC, n_o is calibrated for each block/ sub-basin and n for each reach is calculated as:

$$n_i \; \mathrm{X} n_0(k)[tan \;\; _i / tan \;\; _0(k)] \;\; ^{1/3}$$

n_i is equivalent Manning roughness coefficient of river segment *i*, $tan \;\; _i$ is local topographic gradient and $tan \;\; _0$ is the topographic gradient at the outlet of sub-basin *k*.

III. Drying function parameter (alpha)

Alpha is a parameter which affects the actual evapotranspiration from the root zone. Since knowledge on α is very limited, it is calibrated for each block/sub-basin.

IV. Saturated soil transmissivity (T_0)

T_0 describes the potential rate of lateral flow for a completely saturated soil for a given hydraulic gradient.

For small basins and for basins with relatively similar soil types, constant T_0 value is reasonable. However for larger basins, or even in smaller basins with distinctly different soil distributions in space, assuming constant T_0 is unrealistic. Therefore, in BTOPMC, spatial values of T_0 are considered to be function of soil textures. A linear weighting function is used to get T_0, which is given by

$$T_0 \; \mathrm{X} T_0 Cl \mid U_{cl} \; \Gamma T_0 Sa \mid U_{sa} \; \Gamma T_0 Si \mid U_{Si} \qquad (3.38)$$

where T_0Cl, T_0Sa, T_0Si are T_0 value for clay, sand and silt, and U_{cl}, U_{sa} and U_{si} are the percentages of clay, sand and silt present for each soil type. In BTOPMC, T0 value for clay, sand and silt needs to be calibrated.

V. Maximum root zone capacity (Srmax)

Srmax represents the maximum water holding capacity of the uppermost layer of the soil profile. It represents the plant available soil moisture capacity as well as interception capacity of the canopy.

3.6 Topographic Module

Digital elevation model (DEM) is used in distributed hydrological models for the extraction of drainage network. To ensure and improve the accuracy and reliability of simulation models, drainage networks should

be as accurate as possible to reproduce basin topographic features. The steps involved in DEM processing by BTOPMC model are as follows:

- Removal of pits
- Identification of flow direction
- Calculation of flow gradient and flow contour width
- Calculation of upstream contributing area and Stream network identification.
- Basin delineation

1. Removal of pits

A pit is a point or a set of adjacent points surrounded by neighbors having higher elevations. Flat area is an area, where many cells have the same elevation as its lowest-lying neighbor(s). While some genuine localized depressions in elevation occur within any natural catchment, a majority of depressions at the scale of DEM models are artificial. Pits and flat areas in DEM models are produced by a combination of inaccuracies in the DEM derivation method, and by limitations in the vertical and horizontal resolutions of DEMs. Flow direction cannot be determined in the presence of pits and flat areas introduce the problem of cross-over flow and cause closed flow loops.

Topographic relief tends to decrease from the catchment divide towards the catchment outlet. Based on this observation, the deviation of the corrected elevation of a pit or flat area cell should also decrease towards the catchment outlet away from that of its lowest-lying neighbor. The grid location furthest from the outlet is used as the origin for DEM correction purposes. The model offers automatic pit removal process.

2. Flow direction

Fig 3.4

D8 Method

1	2	3
8		4
7	6	5

The D8 method is a single flow direction algorithm, in which flow from a grid cell takes place to one of its 8 neighbors. In this method flow direction can be diagonal as well as orthogonal.

Two methods are implemented in BTOPMC to assign the direction of flow:

1. Minimum elevation

Flow from a cell takes place to the direction of neighboring cell having lowest elevation among 8 cells.

2. Maximum slope

Flow from a cell occurs in the direction of neighbouring cell having steepest slope (maximum negative gradient) among 8 cells.

3. Flow gradient

Flow gradient is taken equivalent to topographic gradient. It is calculated as

$$\tan \quad X\frac{h\,Zh_0}{L} \qquad (3.39)$$

Where, $\tan$ = flow gradient, $(h-h_0)$ = elevation difference and L = horizontal distance between the centroids of neighbouring cells.

4. Contour width

The contour width for flow is similarly functional on the flow direction (i.e. it differs between orthogonal and diagonal flow directions, as well as with varying grid cell area).

5. Upstream contributing area and stream network identification

Upstream contributing area represents the number of all grids draining through any location. At the catchment divide, the contributing area is simply equal to the area of each grid cell. At the outlet, by definition, the contributing area will be equal to the basin area. A threshold of contributing area value is chosen for stream network identification. All cells with values larger than this threshold are considered as stream channels.

6. Basin delineation

A basin is delineated from all the grid cells which drain through a particular location (outlet). All other grid locations that do not drain to the outlet are excluded from modeling.

7. Basin sub-division

Considering the heterogeneity of a basin, variable parameter values for different sub-basins is more reasonable for a large basin. Hydrology of a certain area behaves independently from that of other areas, such that sub-division is of benefit. Similarly, spatial patterns in geographical or geological properties may

suggest that the basin should be sub-divided to improve predictions.

The basin is sub divided on the basis of drainage network, location of discharge gauging station, number of available gauging station and the basin size and spatial pattern in soil, vegetation and climate.

3.7 Precipitation module of BTOPMC

1. Dataset assessment

1. Check missing values for each gauging stations in the dataset.

2. Exclude gauging stations which consist mainly of missing data.

3. Exclude unusable gauging stations that consist mainly of poor in-filling values.

4. Checking input errors in the dataset.

3.8 Potential Evapotranspiration (PET) module

Shuttleworth-Wallace (SW) model is an extension of Penman-Monteith (PM) model for computing potential evapotranspiration. PM method is a combination method which considers both energy balance and aerodynamic principle. The PM equation is given by

$$PET = \frac{\zeta (R_n - G) + \rho_a C_p (e_s - e_a) / r_a}{\zeta + \gamma (1 + r_s / r_a)} \qquad (3.40)$$

where

ζ = Slope of vapor pressure curve [kPa °C^{-1}]

γ = Psychrometric constant [kPa °C^{-1}]

R_n = Net radiation [MJ m^{-2} day^{-1}]

G = Ground heat flux [MJ m^{-2} day^{-1}]

ρ_a = Density of air at constant pressure [Kg m^{-3}]

C_p = Specific heat of the air [MJ Kg^{-1} °C^{-1}]

e_s = Saturation vapor pressure [kPa]

e_a = Actual vapor pressure [kPa]

r_s = Surface resistance [sm^{-1}]

r_a = Aerodynamic resistance [sm^{-1}]

The PM model is a big leaf model, i.e. it considers vegetation canopy as single uniform cover. Over a large basin, however, the big leaf assumption is rarely valid.

SW model is applicable for sparse vegetation, which considers two coupled sources in a resistance network: the transpiration from vegetation and the evaporation from substrate soil.

The total evapotranspiration is expressed as:

$$^{a}ET = C_c ET_c + C_s ET_s \quad (3.41)$$

Where,

ET = Total evapotranspiration [mm day^{-1}]

^{a} = Latent heat of water vaporization [MJ kg^{-1}]

ET_c = Transpiration from canopy [mm day^{-1}]

ET_s = Evaporation from soil [mm day^{-1}]

C_c and C_s = Weighting coefficients

$$ET_c = \frac{\Delta (R_n - G) + (\rho_a c_p (e_s - e_a) / r_a^c)(R_n^s - G) / (r_a^a + r_a^c)}{\Delta + \gamma (1 + r_s^c / r_a^c)} \quad (3.42)$$

$$ET_s = \frac{\Delta (R_n - G) + (\rho_a c_p (e_s - e_a) / r_a^s)(R_n - R_n^s) / (r_a^a + r_a^s)}{\Delta + \gamma (1 + r_s^s / r_a^c)} \quad (3.43)$$

where

R_n = net radiation at reference height [MJ m^{-2} day^{-1}]

R_n^s = net radiation at substrate soil surface [MJ m^{-2} day^{-1}]

G = substrate soil heat flux [MJ m^{-2} day^{-1}]

e_s = Saturation vapor pressure [kPa]

e_a = Actual vapor pressure [kPa]

ζ = Slope vapor pressure curve [kPa °C^{-1}]

¥ = Psychrometric constant [kPa °C^{-1}]

° = Mean air density [kg m^{-3}]

c_p = Specific heat of moist air [MJ kg^{-1} $^oC^{-1}$]

r_s^c = Bulk stomatal resistances of canopy [sm^{-1}]

r_a^c = Boundary layer resistances of canopy [sm^{-1}]

r_a^s = Aerodynamic resistances between soil and canopy [sm^{-1}]

r_a^a = Aerodynamic resistances between canopy and reference height [sm^{-1}]

r_s^s = Surface resistance of soil [sm^{-1}]

$$C_c = \frac{1}{1 + (R_c R_a)/(R_s (R_c + R_a))} \quad (3.44)$$

$$C_s = \frac{1}{1 + (R_s R_a)/(R_c (R_c + R_a))} \quad (3.45)$$

$$R_a = \frac{\zeta + \gamma}{\rho} r_a^a \quad (3.46)$$

$$R_c = \frac{\zeta + \gamma}{\rho} r_a^c + \gamma r_s^c \quad (3.47)$$

$$R_s = \frac{\zeta + \gamma}{\rho} r_a^s + \gamma r_s^s \quad (3.48)$$

SW model is also applicable to compute evapotranspiration from interception (PET0). PET0 is computed by setting two resistance coefficients, r_s^c and r_s^s, to zero.

3.9 Snow and soil freezing module

The calculation of snow accumulation and melt include following processes (Fig. 3.7): (1) snow accumulation, (2) snowmelt, and (3) melt water outflow from a snowpack. Available energy at snow surface is used to melt snow near the surface, and melt water percolates through the snow layer. During the percolation, some portion of melt water will be captured as liquid water content within a void of snow particle, or re-freeze under cold conditions. Finally, melt water reaches the bottom of the snowpack and infiltrates into the soil or flows out to the stream.

Fig. 3.7

Conceptual Image of Major Processes of Snow Accumulation & Snowmelt

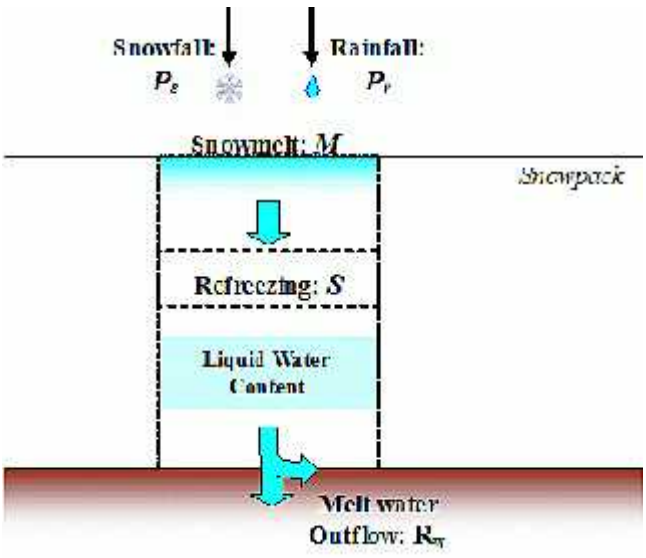

Source: Dulal, 2008

1. Snow accumulation

$P_r \; X P \qquad if \; T_a \mid T_r$ (3.49)

$$P_r = \frac{P(T_a - T_b)}{(T_r - T_b)} \qquad if\ T_b < T_a < T_r \tag{3.50}$$

$$P_r = 0 \qquad if\ T_a \leq T_b \tag{3.51}$$

$$P_s = P - P_r \tag{3.52}$$

where T_a = surface air temperature (ºC), P_r = rainfall, P_s = snowfall, T_r = threshold air temperature above which all precipitation is rainfall, and T_b = threshold air temperature below which all precipitation is snowfall.

2. Snow melt model

Snow melt model in BTOPMC is based on degree day method, which is given by:

$$M = M_f (T_a - T_{base}) \tag{3.53}$$

Where, M is the snow melt (mm day^{-1}); M_f is a degree-day factor (mm $ºC^{-1}$ day^{-1}), T_a is surface air temperature (ºC) and T_{base} is a threshold parameter that represents the temperature above which melt occurs (ºC).

3. Melt water outflow

The melt water outflow from a snowpack, Rw (mm day-1) during the melting season is calculated as

$$R_w = \begin{cases} \frac{M}{1-¤} - P_r & if \quad (M - P_r) > (SWE - P_s) \\ 0 & if \quad (M - P_r) \leq (SWE - P_s) \end{cases} \tag{3.54}$$

where ¤ is a parameter characterizing the maximum liquid water holding capacity of snow, and SWE is amount of snow in water equivalence depth.

When temperatures decrease below T_{base}, the melt water refreezes. The rate of refreezing is calculated as:

$$S = C_{fr} M_f (T_{base} - T_a) \tag{3.55}$$

Where, S is the rate of refreezing (mm day^{-1}) and C_{fr} is a refreezing coefficient.

4 Soil freezing process

There are two conditions for dealing with soil freezing processes in BTOPMC:

1. Air temperature (T_a) ｜ threshold value (T_{freeze})

- Soil is not frozen.
- Infiltration of all water into the root zone, overland runoff occurs when the unsaturated zone becomes saturated

2. Air temperature (T_a) < threshold value (T_{freeze})

- Soil is frozen.
- Only overland flow, no infiltration

4. STUDY AREA

The study area is the Sunkoshi basin in Nepal. The Sunkoshi river system is one of the important components of the Saptakoshi drainage system as it is one of the seven tributaries of the Koshi River basin. It lies in the central northern part of the Nepal in Central Development Region and is one of the river basins with a suitable topography for planning of hydropower schemes. The uppermost portion of the river is known as Bhotekoshi and originates from a Himalayan mountain (5,646 m) on the Tibetan plateau (Ranjit, 2002). It enters Nepal near Tatopani from where it continues south and at Dolalghat, the Indrawati river joins the Sunkoshi.

The watershed under study spreads over border between Nepal and China with about 27% of the total catchment lies in Tibet. Geographically, the study area extends from latitude 27.53^{o}N to 28.37^{o}N and longitude 85.45^{o}E to 86.22^{o}E covering an area of about 4920 km^2 (DHM) at Pachchuwarghat gauging station, including the part of basin in Tibet, China. It mainly covers two districts in Nepal. They are Sindhupalchok and Kavrepalanchok.

The elevation in the basin under study ranges from 602 m at gauging station (DHM) in Pachhuwarghat to 7786 m at high Himalaya. Owing to large differences in the relief, the basin is characterized by diversified climatic patterns. As the snowline is at about an elevation of about 4500 m amsl (Shilpakar, 2009), the precipitation mostly occurs as snow fall above that elevation.

The basin receives an average annual rainfall of about 2300 mm. The average annual runoff of the basin is 1320 mm which accounts for about 57 % of average annual rainfall and remaining 43% accounts for total loss due to evapotranspiration, infiltration, depression storage etc. The major contributions to the flow of the basin are from Indrawati River, which originates in the Himalayan range in the Sindhupalchok district, and from the Bhotekoshi River, which originates from the Himalayan Mountain in Tibet. The Indrawati River flows in southeast direction to meet the Sunkoshi River at Dolalghat. The Bhotekoshi River flows in south direction to meet the Sunkoshi River at Bahrabise. The major landcover of the basin are croplands, croplands/Natural Vegetation Mosaic and open shrub lands.

The location of the basin under study is shown in figure 4.1.

Fig 4.1

Location Map of Sunkoshi Basin in Nepal

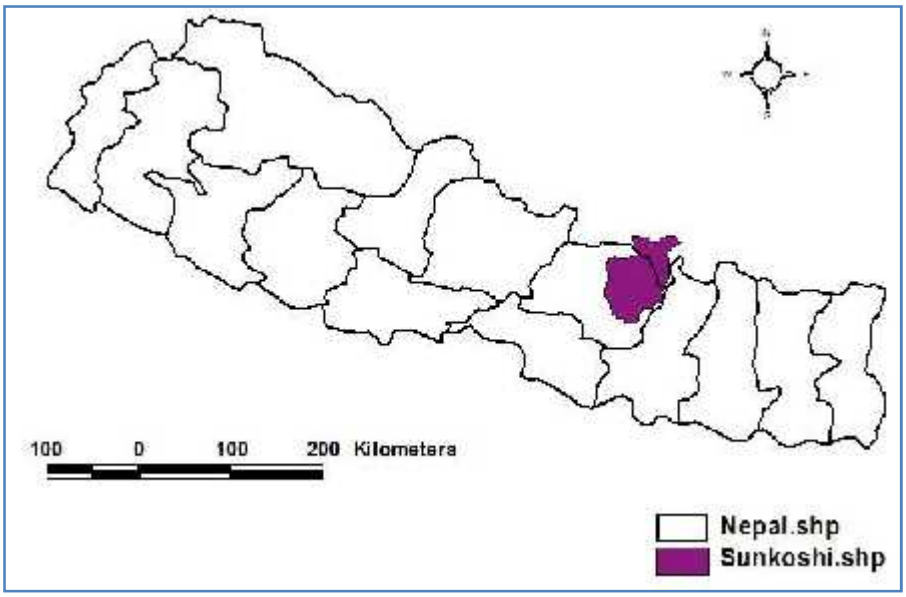

Source: This Study

Fig 4.2

Drainage Network of Sunkoshi River Basin

Source: This Study

The table 4.1 shows the area of the Sunkoshi basin in various districts of Nepal.

Table 4.1

Areas of Sunkoshi Basin Lying in Different Districts of Nepal

S.No.	Districts	Total Area in Sq. Km (Approx.)	Area in Sunkoshi Basin in Sq. Km (Approx.)	% of Total District Area Lying in Sunkoshi Basin
1	Sindhupalchok	2542	2542.00	100.00
2	Kabhrepalanchok	1396	1049.60	75.18
	Total		3591.60	

Source: *This Study*

(The approx. total area of Sindhupalchok and kabhrepalanchok was obtained from the URL www.terraseer.com/data/spacestat_nepal.php)

The basin includes hydropower stations such as Sunkoshi Hydropower Station with 10.05 MW capacity, Upper Bhotekoshi Hydropower Station with 36.00 MW capacity, Indrawati III Hydropower Station with 7.50 MW capacity and Sunkoshi Small Hydropower Station with 2.6 MW capacity (NEA, 2005). However, the Sunkoshi River has a power potential of 4,800 MW (Water Resources Commission). The Melemchi River valley which is the location of a new drinking water project for Kathmandu is also situated in this basin. The Sunkoshi River basin is also susceptible to GLOF events; e.g., a GLOF in 1981 damaged a hydropower plant and many houses along the Sunkoshi River.

The Sunkoshi which is also known as the river of gold is also important from tourism point of view as many tourists practice rafting here enjoying immensely beautiful mountain scenery. Besides, the hot spring in the Upper Sunkoshi River at Tatopani is also popular for the religious baths.

5. METHODOLOGY

The methodology in the study using BTOPMC model basically involved collection of different types of data and processing them into standard formats followed by calibration and validation of the model. Most of these data were available in the public domain of different web sites. For the preparation of standard data format Arc view 3.2/Arc Info, Win BTOPMC preprocessor tool and other different tools of BTOPMC provided by COE-UY (Centre of Excellence- University of Yamanashi). Followings are the steps involved in the study:

1. Collection of data
2. Preparation of DEM
3. Thiessen Polygon generation
4. Preparation of Land cover
5. Reclassification of Land cover
6. Preparation of Soil type
7. Computation of Sr-max
8. Calculation of PET
9. Division of basin into sub basins
10. Calibration of the BTOPMC parameters
11. Validation of the parameters
12. Analysis of the results

5.1 Collection and preprocessing of input data

The input data required to run the model, BTOPMC, falls into two categories. They are spatial data and temporal data. The spatial data includes topographic data, land cover data, soil classification data and NDVI data. These data were collected from different public domains (websites). As they vary with space, they are called spatial data. The hydrological data (discharge) and meteorological data (rainfall and temperature) vary with time series so they are called temporal data. These data were collected from the Department of Hydrology and Meteorology. The DEM, land cover, soil type and vegetation map were represented by grid based maps in ASCII file format prepared from GIS. The temporal data were prepared according to BTOPMC file format. For the calculation of the PET,

the S-W model used the NDVI (Normalized difference vegetation index), monthly average mean daily temperature (^{o} C), monthly average diurnal temperature range (^{o} C), monthly average actual vapor pressure (k Pa), monthly average cloud cover (tenth), monthly average wind speed (m/s) and monthly average extraterrestrial radiation (MJ m^{-2} day^{-1}) and monthly average daylight duration (hr) in the BTOPMC ASCII Volume file format. As BTOPMC requires all the data in its standard form, it was necessary that those data were converted into standard format. The data downloaded from the public domains are:

a) DEM
b) Land Cover
c) Soil Type
d) NDVI
e) Monthly Average Actual Vapor Pressure (k Pa)
f) Monthly Average Wind Speed (m/s)
g) Monthly Average Cloud Cover (tenth)
h) Monthly Average Diurnal Temperature (^{o} C)
i) Monthly Average Extra terrestrial radiation (MJ m^{-2} day^{-1})
j) Monthly Average Mean Daily temperature (^{o} C)
k) Monthly Average Daylight Duration (hr)

The DEM used for topographic analysis were obtained from USGS GTOPO30 data sets. The DEM has a spatial resolution of 1 km from which stream networks were generated using BTOPMC and all related topographic variable required for runoff simulation were calculated. The Thiessen polygon was generated using the preprocessor tool of BTOPMC. The land cover data was represented by IGBP (International Geosphere Biosphere Program) which has classified the global land cover into 17 types at 1 km resolution. The reclassification of the land cover was also done using preprocessor tool of the BTOPMC model. The soil data was represented by FAO (Food and Agriculture Organization) which in conjunction with USDA soil triangle used to compute Srmax.

The NDVI (Normalized Difference Vegetation Index) data were collected from public domain which was monthly data. Later those monthly data were combined together in a single file. Such single file format is called volume file. In volume file format there was information about different months. While making volume file format, BTOPMC Pre- Processing tools were used. The Monthly Average Actual Vapor Pressure, Monthly Average Wind Speed, Monthly Average Cloud Cover, Monthly

Average diurnal temperature, and monthly average mean daily temperature were acquired from CRU climate dataset. The volume file is also prepared for Monthly Average Actual Vapor Pressure, Monthly Average wind speed, monthly average cloud cover, monthly average diurnal temperature range, monthly average daily mean temperature, monthly average daylight duration and monthly average extra terrestrial radiation.

5.2 Calibration

For the basin under study hydrological and meteorological data for the 4-year period from 1994 to 1997 were used to estimate parameters using calibration. The optimization of parameters was done manually. During calibration if the performance is not optimal, parameter values are changed and the simulation is repeated again until the satisfactory result is obtained. The obtained parameters were used to serve following two purposes:

1. To assess the improvement in model performance obtained by using optimized parameters.
2. To validate the model.

There are 5 parameters to be specified in this model which are for runoff generation and for flow routing. Model parameters have physical interpretations, representing the effects of topography (λ), vegetation (Srmax), soil property and moisture (T_o, m, and S_{bar0}) and land cover (n_o) (Ao et al., 2006). Model performance is evaluated by Nash-Sutcliffe Efficiency (N_s) measure and volume ratio (V_r) of simulated to observed discharges.

5.3 Validation

Optimized BTOPMC parameter values were applied to the basin under study for the 4-year period from 1998 to 2001, to obtain daily runoff predictions for the basin. When the validation performance was comparable to performance during calibration, this final set of parameters could be used to extrapolate simulation to other time periods or for different scenario investigations using BTOPMC model.

5.5 Flow Chart of the Methodology

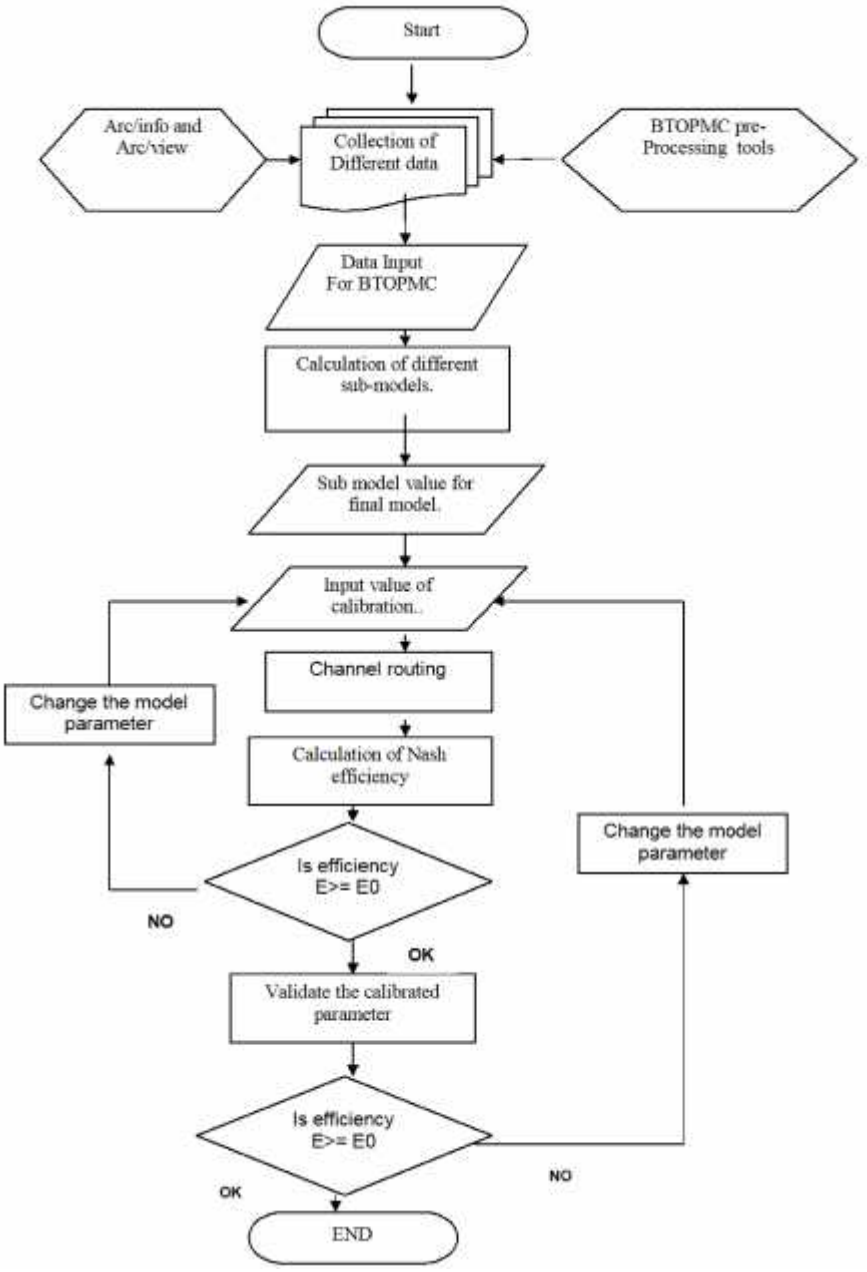

Fig 5.1 Flow Chart of the Methodology of BTOPMC Model

5.4 Filling in Missing Data

The rainfall data were collected from 13 rainfall stations. But, due to large number of missing data, rainfall station at Sarmathang was excluded from the study. Therefore, the study was carried on using rainfall data from 12 rainfall stations. Still three more stations (Paanchkhal, Sangachok, and Tarkeghyang) showed some missing data. In eight years period the rainfall station at Paanchkhal have data missing for 59 days, the rainfall station at Sangachok have data missing for 275 days, the rainfall station at Tarkeghyang have data missing for 16 days. Since missing data were randomly scattered over the year, the missing values were replaced by no rainfall to simplify calculation (Takeuchi et al., 1999).

Meteorological stations (air temperature) were not established in the snow covered region of the basin. There is only one air temperature measuring station in the lower part of the basin (at Paanchkhal), so the temperature data of nearby station at Kyangjing, Langtang which is at 3920 m were used at a point at the same elevation within the basin. The point station having an elevation of 3920 m within the study area was identified using the application - Google Earth.

6 DATA DISCUSSION

The data required to run the model can be divided into two categories. They are spatial data and temporal data. The spatial data includes topographic data, land cover data, soil data and NDVI data. These freely available data were collected from different public domains. As they vary with space they are called spatial data. On the other hand, the hydrological data (runoff) and meteorological data (rainfall and temperature) and climatic data vary with time series so they are called temporal data.

6.1 Spatial Data

The spatial data includes topographic data, land cover data, soil classification data and NDVI data.

6.1.1 Topographic data

A digital elevation model (DEM) is a digital representation of ground surface topography. A DEM can be represented as raster (a grid of squares). The DEMs are commonly built using remote sensing techniques. The DEMs are used often in geographic information systems. It contains the specific elevation values at specific grid point locations. The files can be in either ASCII or binary. In this study the topographic map is represented by grid based map in ASCII file format prepared from GIS.

Fig 6.1

DEM of Sunkoshi River Basin

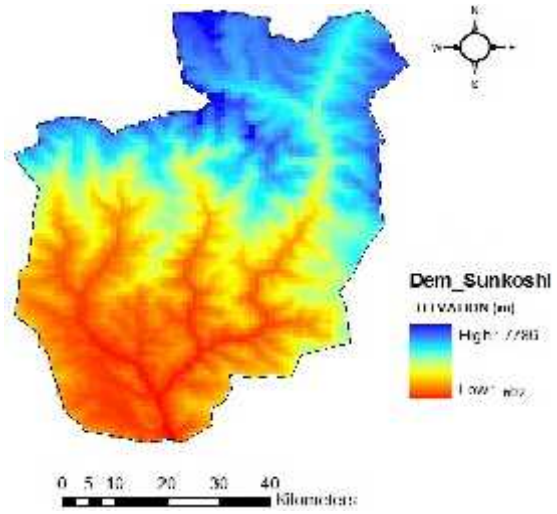

Source: This Study

The above figure (Fig. 6.1) shows that the topography of the study area varies widely from the low lands to higher Himalayas. The elevation of the basin varies from 602 m to 7786 m.

Fig 6.2

Elevation Bands of Sunkoshi River Basin

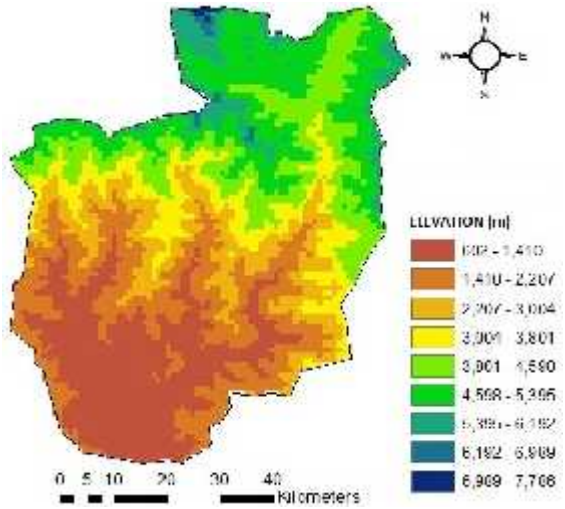

Source: This Study

The above figure (Fig 6.2) shows different elevation bands of the Sunkoshi River basin. These elvation bands have an equal interval of 797 m. However, the first elevation band has an interval of 808 m.

For the purpose of the study, the DEM data of 1 km resolution was downloaded from the website of USGS (United States Geological Survey) which is given below:

http://eros.usgs.gov/#/Find_Data/Products_and_Data_Available/gtopo30_info

6.1.2 Land cover data

A land cover is the physical material at the surface of the earth. The land cover includes grassland, water bodies, bare ground, forests etc. The two primary methods for capturing information on land cover are field survey and analysis of remotely sensed imagery. The land cover data of 1 km pixel resolution can be downloaded from the following URL:

http://edc2.usgs.gov/glcc/glcc_version1.php

The subsetting of data thus obtained was done by the help of “glcc data subset tool”.

The figure shown below is land cover of the Sunkoshi river basin.

Fig. 6.3

Landcover of Sunkoshi River Basin

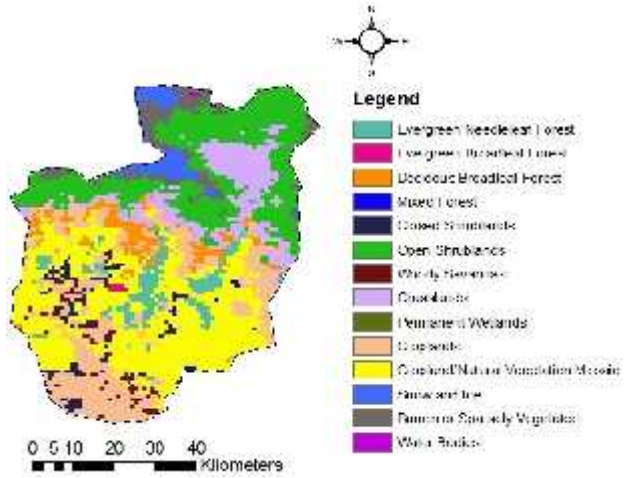

Source: This Study

The IGBP (International Geosphere-Biosphere Programme) has classified the global land cover into 17 types. (See Appendix No a). The IGBP landcover classification of the Sunkoshi River basin is shown in the following table (Table 6.1).

Table 6.1

IGBP Landcover Classification of the Sunkoshi River

ID	Category	Area (%)	New ID	New Area (%)	New Category
1	Evergreen Needle Leaf Forest	5.02	1	9.93	Deep Rooted
2	Evergreen Broad Leaf Forest	0.17			
4	Deciduous Broadleaf Forest	4.53			
5	Mixed Forests	0.21			
6	Closed Shrub lands	2.56	2	35.8	Shallow Rooted (Grassland)
7	Open Shrub lands	21.89			
8	Woody Savannas	1.40			
10	Grasslands	9.95			
12	Croplands	16.49	3	19.97	Shallow Rooted and Irrigated
14	Cropland/Natural Vegetation Mosaic	29.02			
11	Permanent Wetlands	0.02	4	8.77	Impervious
15	Snow and Ice	3.48			
16	Barren or Sparsely Vegetated	5.21			
17	Water Bodies	0.06			

Fig 6.4

Reclassified Landcover of Sunkoshi River Basin

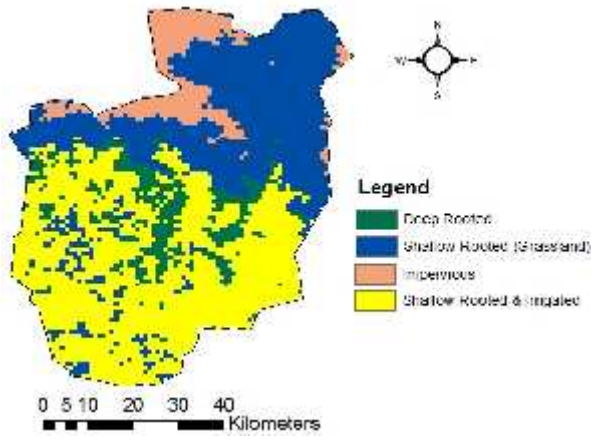

Source: This Study

From above figure (Fig. 6.3) and Table 6.1, it is obvious that the major land cover of the basin is croplands then follows shrub lands and then woody savannas. The original 17 class was reclassified into 4 class named deep rooted (DR), shallow rooted (SR), shallow rooted and irrigated deep rooted (SRI), and impervious (IMP) which is shown in Fig 6.4. The Land cover classification data are used for calculating maximum soil moisture storage capacity of root zone over the basin under study.

6.1.3 Soil Data

The soil properties of the catchment were obtained using the FAO (Food and Agriculture Organization) soil map having spatial scale of 5 km resolution. The soil map (Fig 6.5) of the Sunkoshi River Basin shows different types of soil which are represented by different soil IDs. There are altogether 3 soil classes in the basin which are represented as the content percentage of sand, silt and clay.

The soil data were downloaded in vector form from the following URL:

http://www.fao.org/geonetwork/srv/en/metadata.show?id=14116

Using ArcView GIS 3.2 the downloaded data was converted into raster and then sub setting is done using spatial analyst.

Fig 6.5

Soil Map of Sunkoshi River Basin

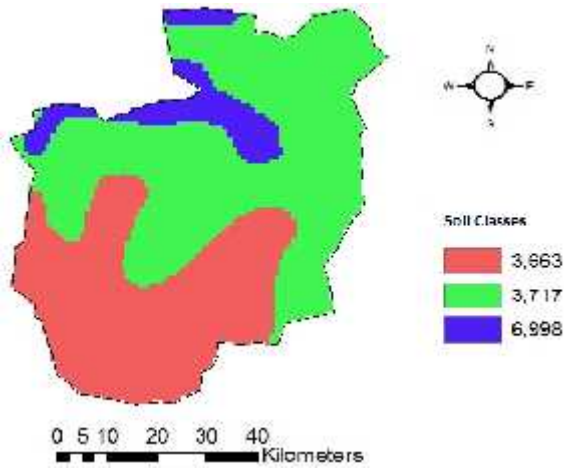

Source: This Study

The soil map of the Sunkoshi River Basin shows different types of soil which are represented by different soil IDs. There are altogether 3 soil classes in the basin which are represented as the content percentage of sand, silt and clay.

The soil data were downloaded in vector form from the following URL:

http://www.fao.org/geonetwork/srv/en/metadata.show?id=14116

Using ArcView GIS 3.2 the downloaded data was converted into raster and then sub setting is done using spatial analyst.

Table 6.2

Percentage of clay, sand and silt

Soil ID	Clay %	Sand %	Silt %
3663	26.899	45.8886	27.2125
3717	24.1414	56.6856	19.1731
6998	33	34	33

These soil classes were transferred to USDA soil classification, and two types of soil were found. They were sandy clay loam and clay loam. The USDA (United States Department of Agriculture) soil triangle was used to find the classes of soil according to USDA classification. The figure 6.6 represents the USDA soil triangle.

Fig 6.6

USDA Soil Classification Triangle

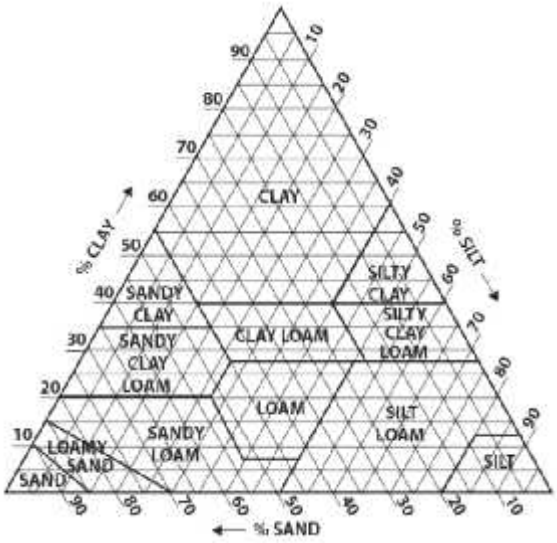

Source: CREEW, 2008

The FAO soil classes are used to calculate T_o (Saturated soil transmissivity) over the basin. The values of T_o for sand, silt and clay were calibrated. In BTOPMC model, spatial values of T_o are considered to be function of soil textures. The transferred USDA classes are used for assessing the maximum soil moisture storage capacity of root zone (Srmax).

6.1.4 Srmax

The Srmax represents the maximum water holding capacity of the uppermost layer of the soil profile. In this study, the Srmax parameter is calculated for each grid using the soil and land cover properties of that grid cell which is given as follows:

$Srmax = RD \times (\theta_{fc} - \theta_{wp})$

Where,

θ_{fc} is the field capacity of the top soil,

θ_{wp} is the moisture content at wilting point of the top soil layer in each grid and

RD (m) is the root depth for each land cover class.

The Srmax is calculated by using Srmax calc. tool. The input for which are land cover (ASCII raster), root depth, soil type (ASCII raster), and theta. The output is obtained as Srmax (ASCII raster). The values of root depth for different types of land cover is shown in Table 6.3.

Fig 6.3

Root Depth for IGBP Land Cover Classification

ID	Category	Root Depth (m)
1	Evergreen Needle Leaf Forest	2.5
2	Evergreen Broad Leaf Forest	2.5
3	Deciduous Needle Leaf Forest	2.5
4	Deciduous Broadleaf Forest	2.5
5	Mixed Forests	2.0
6	Closed Shrub lands	1.0
7	Open Shrub lands	1.0
8	Woody Savannas	1.0
9	Savannas	1.0
10	Grasslands	0.5
11	Permanent Wetlands	1.0
12	Croplands	0.7
13	Urban and Built-Up	0.001
14	Cropland/Natural Vegetation Mosaic	1.0
15	Snow and Ice	1.0
16	Barren or Sparsely Vegetated	1.0
17	Water Bodies	0.001

Source: CREEW, 2008

The value of θ_{fc} and θ_{wp} was found out by the help of USDA soil class. The table 6.7 represents θ_{fc} and θ_{wp} according to USDA soil classification.

Table 6.4

θ_{fc} and θ_{wp} for Sunkoshi River Basin

Soil ID	USDA Classification	θ_{fc}	θ_{wp}
3663	Sandy Clay Loam	0.255	0.068
3717	Sandy Clay Loam	0.255	0.068
6998	Clay Loam	0.318	0.075

Source: This Study

After preparing all necessary input data for Srmax, the Srmax for Sunkoshi basin was calculated using the Srmax calc. tool and it was found that the value of Srmax ranges from 0 to 0.468. The figure below shows the Srmax of Sunkoshi basin.

Fig 6.7

Srmax of Sunkoshi River Basin

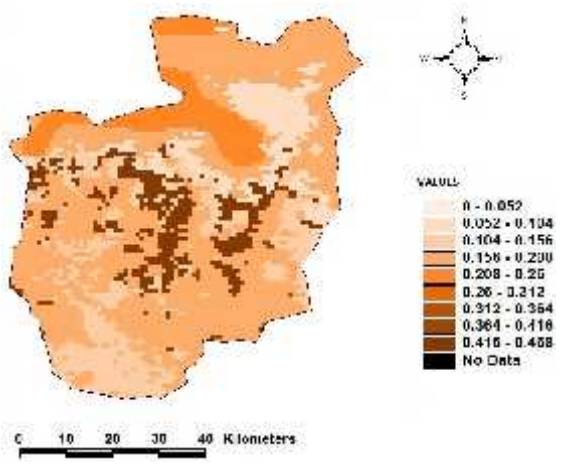

Source: This Study

6.1.5 NDVI data

The basic index for measuring the 'greenness' of the earth's surface is the Normalized Difference Vegetation Index (NDVI), which is basically a calculation of the differences between AVHRR channels 1 and 2. A reasonable estimation of the density and coverage of green vegetation can be determined by measuring how green the earth's surface is.

NDVI values are unitless. Values of NDVI can range from -1.0 to +1.0. The NDVI values greater than 0.1, generally denote increasing degree in greenness and intensity of vegetation. The Values

between 0 and 1 are commonly characteristic of rocks and bare soil and values less than 0 sometimes indicate clouds, rain and snow.

The NOAA NDVI average monthly data set at 8 km resolution was used. The average monthly data from the year 1994 to 2001 was used for study. The data set was downloaded from the following URL:

http://dis.c.gsfc.nasa.gov/interdisc/readmes/pal_ftp.shtml

First of all the subsetting of the global data set was done using NDVI subsetting program (subset_pal_ndvi). Then a control file was prepared in a notepad. The control file lists the path of the file for combining into one file, layer by layer. Finally, it was converted into volume file using the program volume_conversion.

The NDVI data was used for the estimation of PET over the basin under study by the model.

6.2 Temporal Data

The temporal data includes hydrological data and meteorological data.

6.2.1 Hydrological Data

For the purpose of the study the daily observed discharge data at Pachhuwarghat stream gauging station were used for calibration and validation of the model. It is a point data and obtained from the Department of Hydrology and Meteorology, Nepal. The daily observed discharge data covered the period of 1994 to 2001. These data were prepared in standard format of BTOPMC using a text editor (Notepad).

6.2.2 Meteorological Data

The meteorological data includes daily average precipitation and daily average temperature data. These are also point data obtained from the Department of Hydrology and Meteorology, Nepal. For the purpose of the study, daily precipitation data at 12 rainfall stations throughout the basin were collected. The daily precipitation data covered the period of 1994 to 2001. These data were also prepared in standard format of BTOPMC using a text editor (Notepad). Then the text format was used to prepare Thiessen Polygon of rainfall which was used by the BTOPMC model. The Thiessen Polygon of rainfall is shown in fig 6.7.

Fig 6.8

Thiessen Polygon of Rainfall in Sunkoshi River Basin

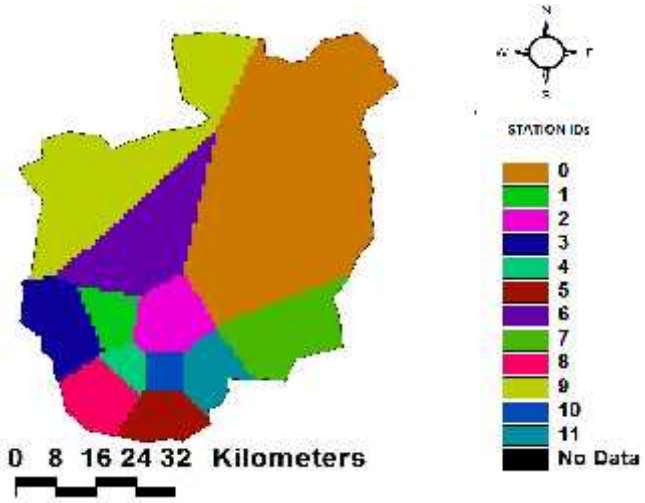

Source: This Study

The meteorological stations used in the Sunkoshi basin were given in the following table.

Table 6.5

Rainfall Stations Used for the Study of Sunkoshi River Basin

IDs	Station Index	Name	District	Elevation	Latitude	Longitude
1	1006	Gumthang	Sindhupalchok	2000	27.866	85.866
2	1008	Nawalpur	Sindhupalchok	1592	27.8	85.61
3	1009	Chautara	Sindhupalchok	1660	27.783	85.716
4	1018	Baunepati	Sindhupalchok	845	27.783	85.566
5	1020	Mandan	Kavrepalanchok	1365	27.7	85.65
6	1023	Dolalghat	Kavrepalanchok	710	27.633	85.716
7	1025	Dhap	Sindhupalchok	1240	27.916	85.633
8	1027	Bahrabise	Sindhupalchok	1220	27.783	85.9
9	1036	Panchkhal	Kavrepalanchok	865	27.683	85.633
10	1058	Tarkeghyang	Sindhupalchok	2480	28	85.55
11	1062	Sangachok	Sindhupalchok	1327	27.7	85.716
12	1063	Thokarpa	Sindhupalchok	1750	27.7	85.783

Source: DHM

6.3 Potential Evapotranspiration (PET)

In order to calculate PET, the global datasets of different meteorological data, CRU (Climate Research Unit) dataset, were used. The CRU TS 2.0 provides monthly time series data of the

monthly mean temperature, monthly mean diurnal temperature range, monthly mean cloud cover, monthly mean actual vapor pressure and monthly mean wind speed. The CRU data sets at 10 km resolution were extracted for Sunkoshi river basin using program "subset_cru1". While subsetting, the unit conversion of *0.1 is used for temperature, diurnal temperature range, cloud cover and wind whereas the unit conversion of *0.01 is used for actual vapor pressure. The CRU TS 2.0 data set was downloaded from the following URL:

http://www.ipcc-data.org/obs/get_30yr_means.html

The extraterrestrial radiation and sunshine hours can be calculated from the Julian date and the location latitude. The program "calc_extra_pds" was used for this computation. Then control files were prepared in a Notepad. The control file lists the path of the file for combining into one file, layer by layer. Finally, they were converted into volume file using the program volume_conversion. Finally, all the necessary input files (DEM, Land Cover, NDVI, Mean Daily Temperature, Diurnal Temperature Range, Cloud Cover, Vapor Pressure, Wind Speed, Extraterestrial Radiation and Possible Duration of Sunshine) were fed into the PET Model (YHyM/PET). From the model, three types of files were obtained as output on the monthly basis. Those three types of files were the files with extension .lai (leaf area index), .pet (potential evapotranspiration from root zone) and .pet0 (potential evapotranspiration from interception). The figure 6.8 shows the PET from root zone of the Sunkoshi River Basin in Dec, 1994.

Fig. 6.9

PET from root zone of Sunkoshi River Basin in December (1994)

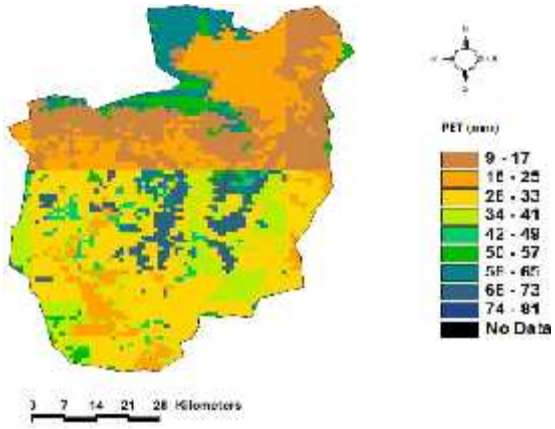

Source: This Study

The average monthly PET from root zone of the Sunkoshi River Basin in December, 1994 is about 31.86 mm. Similarly, the average monthly PET from interception of the basin in same month is

found to be 182.60 mm. The figure 6.9 shows PET from interception (pet0) of the Sunkoshi River basin in December, 1994.

Fig 6.10

PET from Interception of Sunkoshi River Basin in December (1994)

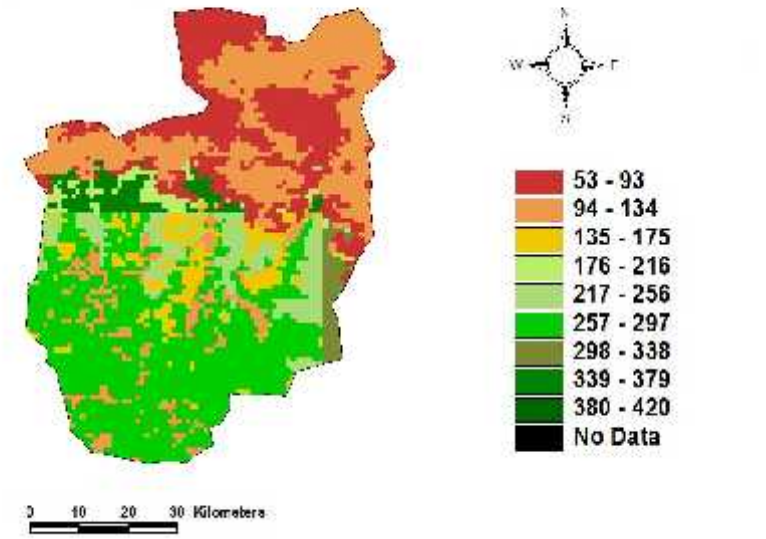

Source: This Study

6.4 Snow Accumulation/Melt

This river originates from the Himalayas and carries snow fed flows with significant discharge even in dry season. The Snow module is based on a simple degree-day method. It has simulated daily snow accumulation and ablation using daily rainfall and air temperature as input. Measured precipitation is partitioned into rain and snow by the air temperature above or below a threshold. Pure snowfall occurs at air temperature below the first threshold, pure rainfall above the second threshold and in between it is sleet. During snow accumulation, snowfall is added to the snow pack. Liquid-water in excess of the capacity in the snow pack will percolate through the snow layer and becomes melt-water outflow.

Fig 6.11

Monthly Variation in Snow Cover Area of Sunkoshi River Basin (1994)

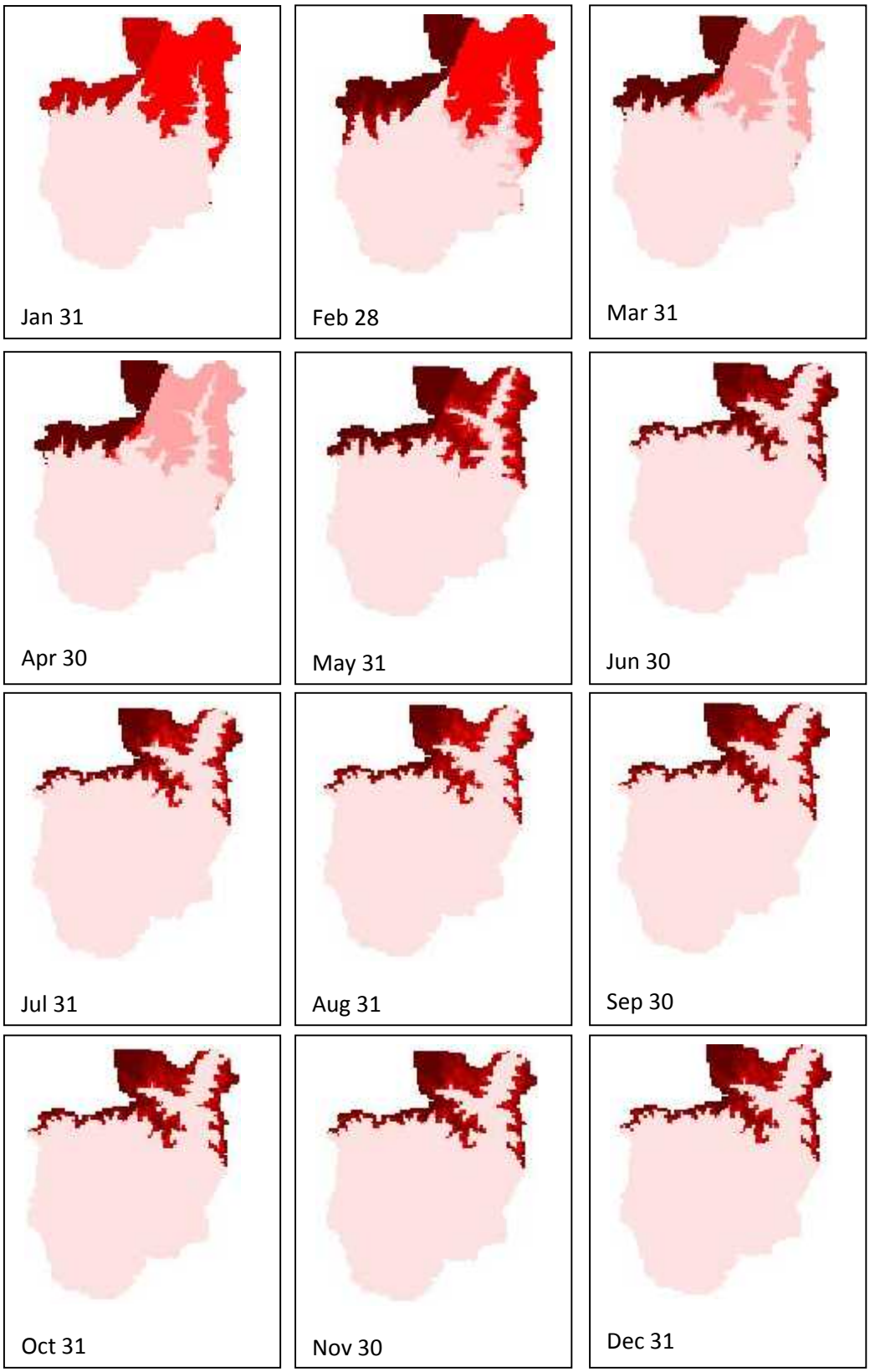

The figure 6.11 shows monthly variation in snow cover region of the Sunkoshi River Basin under study as given by the model. During winter the snow accumulates as a result of snowfall and the snow cover area increases whereas during summer it decreases due to melting as a result of rising air temperature.

Northern hemispheric weekly snow cover charts and global monitoring of the Himalayan snow cover data carried out by NOAA show that the snow cover is minimum in August and maximum in February (Bahadur, 1992).

The fig 6.11 also shows the similar results. The snow cover area was maximum in February because of precipitation in the form of snow and minimum in August because of melting. In fig 6.11 the snow cover was indicated by red color with the higher snow amount with darker red color.

The monthly variation in snow cover area of the Sunkoshi River Basin was calculated in percentage only for the year 1994. The snow cover area was observed to be highest in February i.e., 47.78 % and lowest in August i.e., 18.09 %. The table 7.7 shows monthly variation of snow cover area (in percentage) of the Sunkoshi River Basin in the year 1994 and fig 7.10 is the graphical representation of the same as given by the model.

Table 6.6

Monthly variation in Snow Cover Area in Percentage (1994)

Months	Snow Cover Area (%)
Jan	36.11
Feb	47.78
Mar	34.73
Apr	37.43
May	27.48
Jun	20.20
Jul	18.11
Aug	18.09
Sep	20.33
Oct	24.76
Nov	27.48
Dec	23.46

Source: This Study

Fig 6.12

Monthly Variation in Snow Cover Area in Percentage (1994)

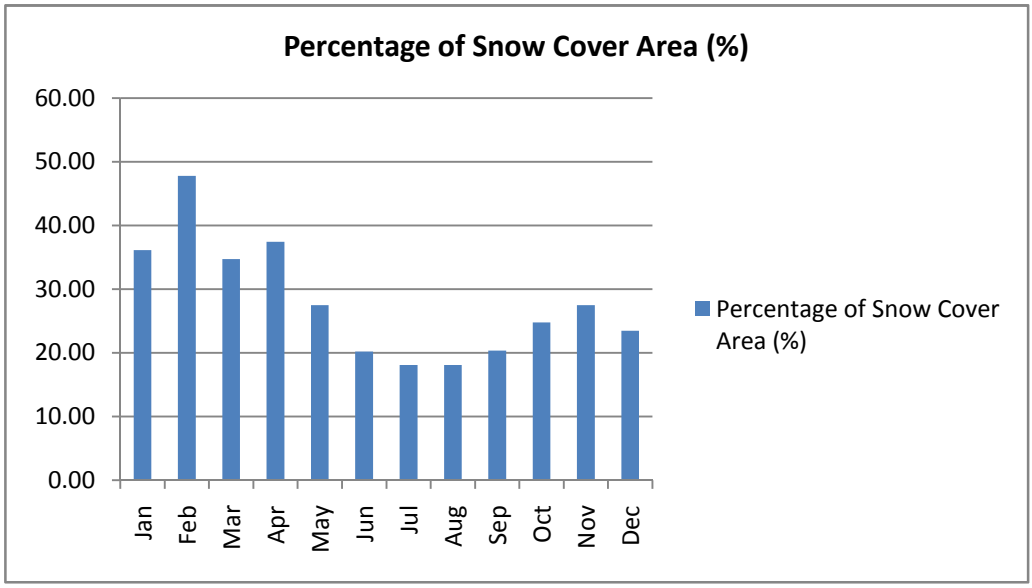

7. RESULTS AND DISCUSSION

The BTOPMC model is capable of generating the simulation results at any time anywhere in the basin. In this application, the model was simulated using the observed discharge at the gauging station in Pachhuwarghat. Simulations were carried out for the years 1994, 1995, 1996, 1997, 1998, 1999, 2000 and 2001. The model was calibrated for the years 1994, 1995, 1996 and 1997 and validated for the years 1998, 1999, 2000 and 2001.

7.1 Performance Indicators

For successful calibration it is necessary to focus on the following objective functions:

a. Nash-Sutcliffe Coefficient (Nash and Sutcliffe, 1970)

The Nash-Sutcliffe Coefficient is widely used indicator of model performance for the hydrological model. Therefore determining the Nash Efficiency of both results can do the quantitative justification of both calibration and validation. The Nash-Sutcliffe Efficiency is given by the following formula:

$$Efficiency = 1 - \frac{\sum_{i=1}^{N}(Qobs_i - Qsim_i)^2}{\sum_{i=1}^{N}(Qobs_i - \overline{Qobs})^2}$$

Where,
Qobs = observed discharge,
Qsim = simulated discharge,
N = the total number of time steps
$\overline{Qobs}$ = the mean of observed discharge.

b. Overall Volume Error

The Nash-Sutcliffe Efficiency is more biased towards high flows i.e. it gives less weight to low flow errors. Therefore to check the mass balance, another measure called the overall volume error is also computed which is given by the following formula.

$$OVE = \sum_{i=1}^{N}(Qobs_i - Qsim_i)$$

In terms of ratio, $Qobs_i/Qsim_i$ is used in BTOPMC. Or, the volume bias (VB) can be calculated using the formula, $VB = \frac{\sum(Qsim - Qobs)}{\sum Qobs}$

7.2 Calibration and Validation

Model calibration is the process by which the values of model parameters are identified to use in a particular application. The identified parameters are then used in validation where, using independent input time series data, observed responses are compared with predicted responses. Validation is conducted to check the validity of the calibrated parameter set. If the calibrated parameter set is physically sound, the validation results should be same as calibrated results or better. After validation, the model can be used to simulate long period to make future prediction. The criteria set for evaluation of the model are shown in the table 7.1:

Table 7.1

Criteria for Evaluation of the Model

	NSE	VB
Excellent	Above 85 %	Below 5 %
Very Good	65 % - 85 %	5 % - 10 %
Good	50 % -65 %	10 % - 20 %
Poor	20 % - 50 %	20 % - 40 %
Very Poor	Below 20 %	Below 40 %

Source: (Henriksen et al., 2003)

In this study the model was calibrated twice with snow module; firstly using the option "calculate using soil and land cover data" (i.e., without reclassification) and secondly using the option "calibrate" (i.e., with reclassification) for the computation of Srmax for 4 years from 1994 to 1997 with the simulation time step of 1 day.

Fig 7.1

Basin Sub-division

Source: This Study

For simulation the whole basin was divided into 5 sub basins and the outlet was taken at the Pachhuwarghat gauging station so the parameters of sub basin 0, 1, 2, 3 and 4 affect the simulation result. The figure 7.1 shows basin subdivision with basin ID.

The BTOPMC parameters were calibrated manually by Trial and Error method. The calibration of parameters using trial and error method was a very time consuming task. But, it was necessary due to the immeasurability of model parameters. This immeasurability is due to lacking exact physical meaning, measurement techniques and/or the application to a particular model scale (Ao et al., 2006).

Table 7.2

Optimized Model Parameters from Manual Calibration

Parameter	Unit	Sub-basin 0	Sub-basin 1	Sub-basin 2	Sub-basin 3	Sub-basin 4
n_0	-	0.11	0.15	0.17	0.18	0.21
m	*m*	0.18	0.15	0.11	0.09	0.06
α	*m*	0.008	0.012	0.014	0.014	0.017
SDbar	*m*	0.001	0.007	0.014	0.014	0.014
Srmax-DR	*m*	0.022	0.022	0.022	0.022	0.022
Srmax-SR	*m*	0.018	0.018	0.018	0.018	0.018
Srmax-SRI	*m*	0.012	0.012	0.012	0.012	0.012
Srmax-IMP	*m*	0.0001	0.0001	0.0001	0.0001	0.0001
T_0 - Clay	m^2/h	0.4				
T_0 - Sand	m^2/h	0.9				
T_0 - Silt	m^2/h	0.6				
dl	-	3				
dt	-	3				

Table 7.3

Calibrated Parameters for soil freezing and snow module

Parameters	Unit	Value
Soil Freezing Threshold Temperature	deg. C	0
Snow accumulation parameters: T_b & T_r		
Threshold temp. below which all precipitation is snow (T_b)	deg. C	-2
Threshold temp. above which all precipitation is rainfall (T_r)	deg. C	2
Degree day factor (M_f)	mm day^{-1} $^0C^{-1}$	7
Threshold temperature of snow melt (T_{base})	deg. C	0.5
snow pack yield parameter (ϕ)		0.5
refreezing coefficient (C_{fr})	mm/day	0.05

The Model parameters have physical interpretations, representing the effects of topography, soil properties and moisture (T_0, m and SD_{bar}), vegetation (Srmax), and land uses (n_0) (Ao et al., 2006). Similarly, n_0, dt and dl are used in the Muskingum-Cunge flow routing module. The final optimized parameters obtained from the manual calibration were presented in table 7.2 and 7.3.

7.2.1 Calibration and Validation using the Option "Calculate using Soil and Land Cover Data"

When the model was calibrated without using the option "calculate using soil and land cover data" for Srmax computation, the Nash Efficiency for the model was found to be 81.41% with the volume ratio of 89.35 % and volume bias of -10.65 %. The hydrograph for the calibration of the model is shown in figure 7.2

Fig 7.2

Hydrograph from Calibration of the Model using the Option "Calculate using Soil and Land Cover Data"

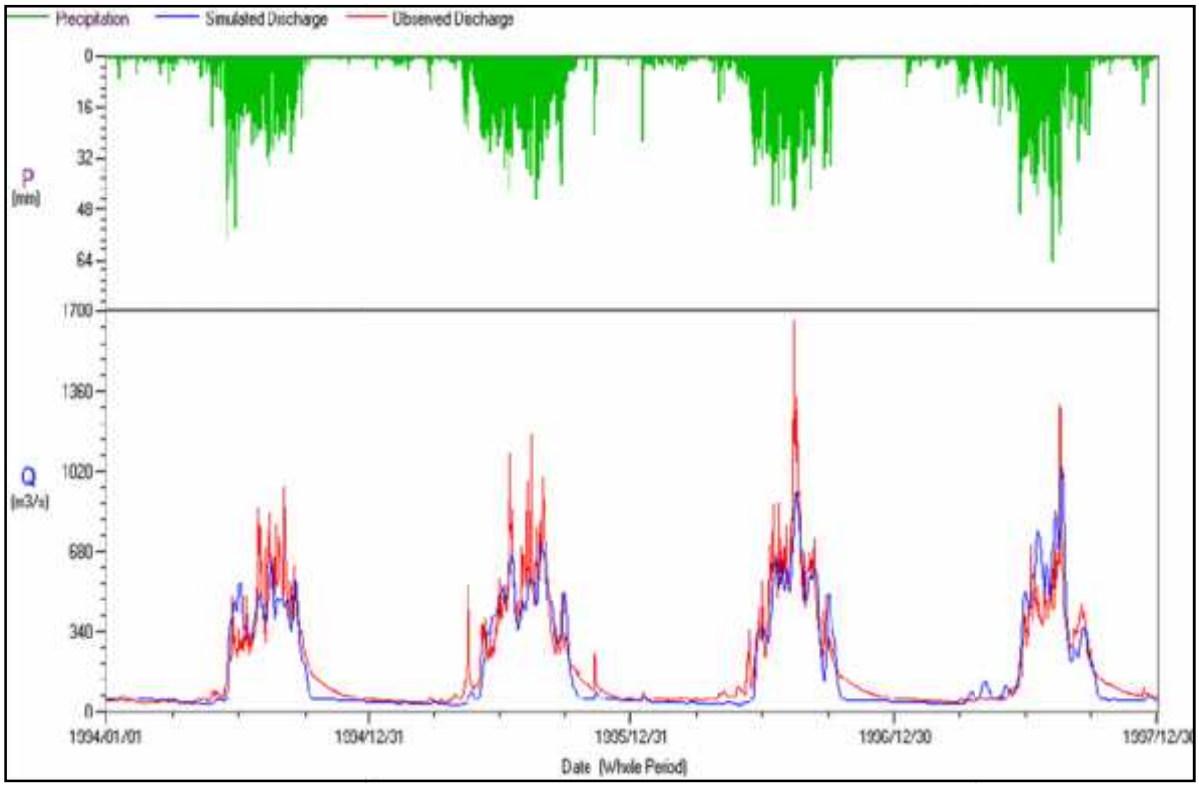

Comparison of observed and the simulated hydrograph showed that the simulated runoff is underestimated than the observed runoff. The low flows (dry season flows) were somewhat well captured. The highest peak flows were underestimated. However, the model has reproduced most parts of the observed hydrograph and simulated well the seasonal and annual variations in runoff. The flow in Aug 13, 1996 was recorded 1670 m^3/s, the highest during the study period, and which

might be due to continuous rainfall in the part of basin that lies in Nepal as a result of monsoonal effect.

After the model was calibrated, it was validated by comparing the simulated flows for the years 1998, 1999, 2000 and 2001 and observed flow for the same years. The hydrograph for validation of the model is presented in the figure 7.3.

Fig 7.3

Hydrograph from validation of the Model using the Option "Calculate using Soil and Land Cover Data"

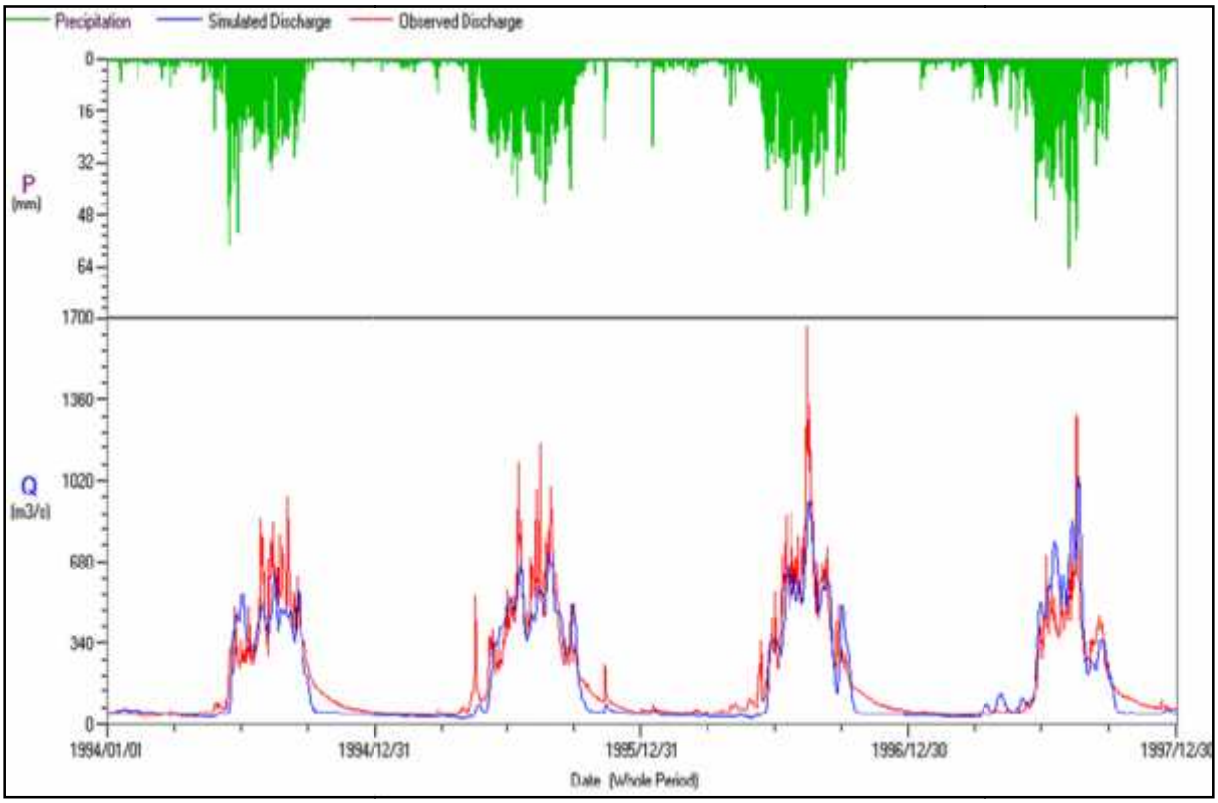

The validation period was taken from start of 1998 to end of 2001. The Nash Efficiency achieved was 82.87 % with volume ratio achieved was 101.05 % and volume bias of 1.05 %. The Nash Efficiency as well as volume ratio was very good but still the simulated high peak was underestimated than the observed high peak.

From the results, the model performance at the gauging station both in calibration and validation is acceptable. Therefore the model can be successfully applied for hydrological simulations in the Sunkoshi river basin.

7.2.2 Calibration and Validation using the option "Calibrate"

When the model was calibrated using the option "calibrate" for Srmax computation, the Nash Efficiency for the model was found to be 81.67 % with the volume ratio of 99.67 % and volume bias of - 0.32 %. The hydrograph for the calibration of the model is shown in figure 7.4. Although the Nash Efficiency was good and the low flows were well captured the high peaks were underestimated.

Fig 7.4

Hydrograph from Calibration of the Model using the option "Calibrate"

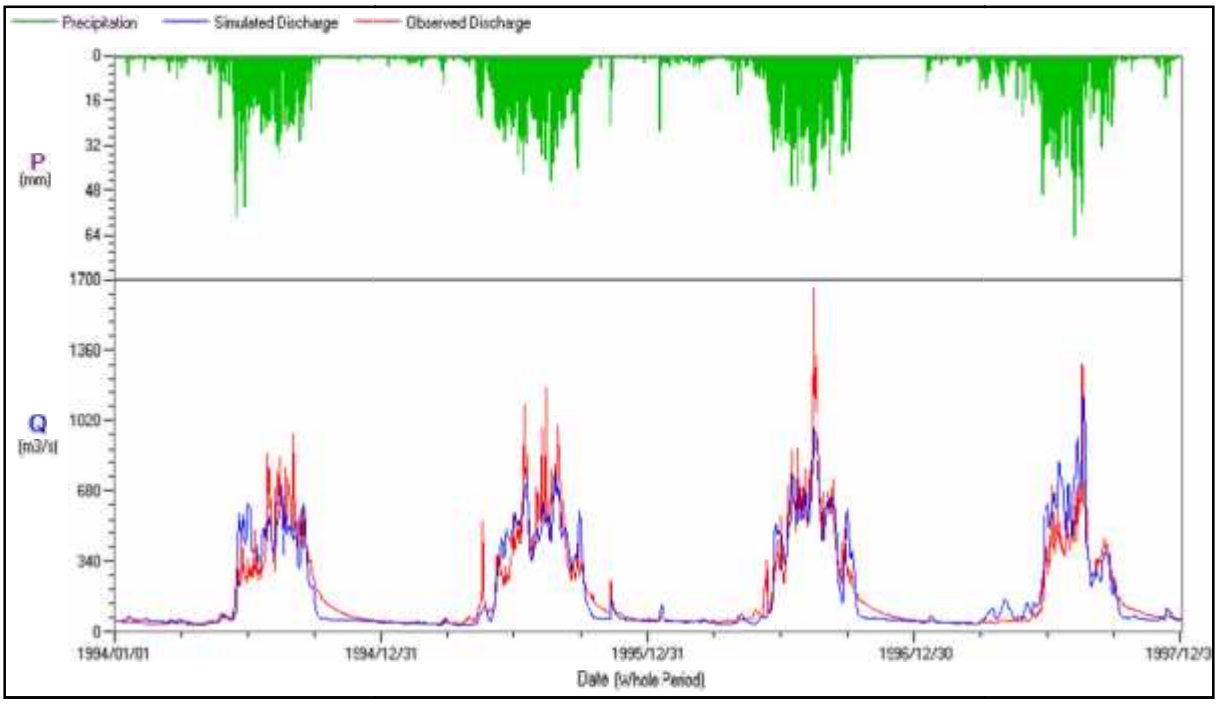

For simulation the whole basin was divided into the same 5 sub basins (see fig 7.1) with outlet at the Pachhuwarghat gauging station so the parameters of sub basin 0, 1, 2, 3 and 4 affect the simulation result. The optimized parameters used were same as used in calibrating the model using the option "calculate using soil and land cover data" for Srmax computation which are presented in table 7.1 and 7.2.

After the model was calibrated, it was validated by comparing the simulated flows for the years 1998, 1999, 2000 and 2001 and observed flow for the same years. The Nash's Efficiency of 82.01 % with volume ratio of 108.58 % and volume bias of 8.59 % were obtained from validation. The Nash Efficiency was very good. The hydrograph for validation of the model is presented in the figure 7.5. The comparison of the simulated and the observed hydrograph showed that the low flows being well captured and high peaks were underestimated than the actual high peaks.

Fig 7.5

Hydrograph from Validation of the Model using the Option "Calibrate"

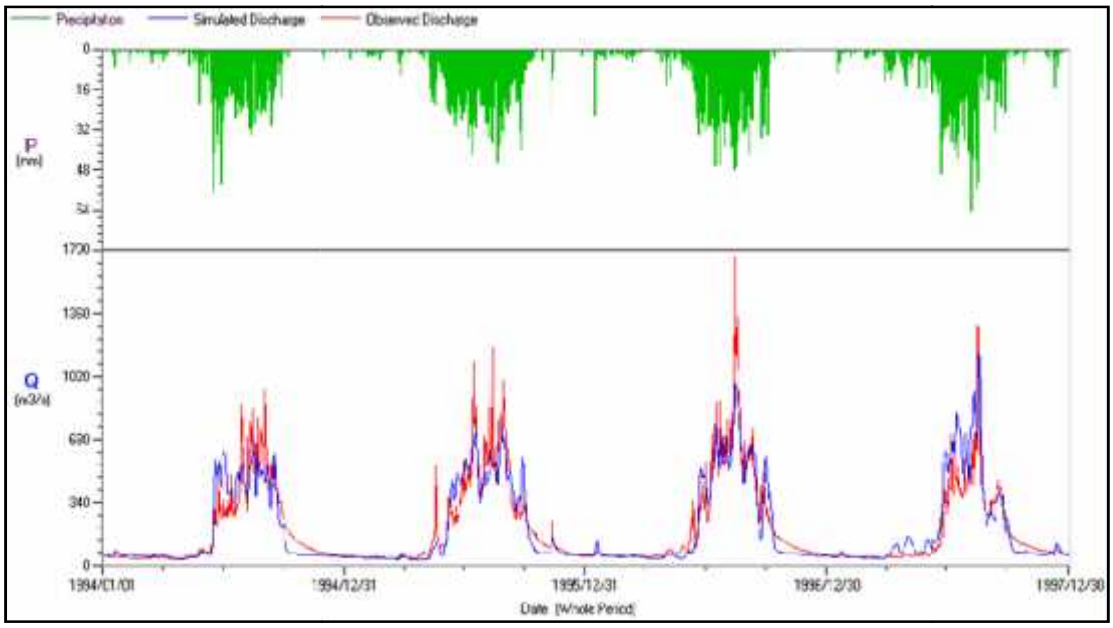

The Nash efficiency of the river basin under study was found to be somewhat consistent in both when calculated using either calibrate option or calculate using soil and land cover data. The comparison of Nash efficiency using both options for Srmax computation is shown in table 7.3.

Table 7.4

Comparison of NSEs

	NSE using "calculate using soil and land cover data"	NSE using "calibrate" option
Calibration	81.41 %	81.67 %
Validation	82.87 %	82.01 %

7.2.3 Significance of Model Parameters

The BTOPMC model uses parameters related to soil and land cover such as saturated soil transmissivity (T_0), decay factor of transmissivity (m), drying function parameter (α) and maximum root zone capacity (Srmax). It uses routing parameters such as block average roughness coefficient (n_0), time step division for routing (dt), and length step division for routing (dl). The soil freezing and snow module uses parameters such as soil freezing threshold temperature (T_{thd}), degree day factor (M_f), threshold temperature for snowmelt (T_{base}), snow pack yield parameter (phi), refreezing coefficient (C_{fr}), threshold temperature above which all precipitation is snow (T_b), and threshold

temperature above which all precipitation is rainfall (T_r). The identification of optimized model parameters is very important to achieve best model outputs. In the BTOPMC model, the trial and error method is used to optimize the model parameters by manual calibration.

The saturated transmissivity of soil (T_0) varies with soil classes. In BTOPMC the T_0 is calibrated for clay, sand and silt. The T_0 contributes in infiltration and base flow generation. The higher values of T_0 increases base flow and decreases high flow whereas the lower values of T_0 decreases base flows and increases high flows. The highest value of T_0 was observed in the case of sand which was 1.1 m^2/h and the lowest in the case of clay which was 0.4 m^2/h. The T_0 of silt was observed to be 0.6 m^2/h.

The transmissivity decay factor (m) controls the decay of the hydrograph. Larger the value of m, faster will be the decay of the hydrograph thereby reducing the volume of flow and smaller the value of m slower will be the decay of the hydrograph thereby increasing the volume. The average value of m in the Sunkoshi river basin was observed to be 0.118 m.

The maximum storage capacity at root zone (Srmax) represents the maximum water holding capacity of the uppermost layer. The uppermost layer of the soil profile includes root zone plus canopy cover. The Srmax parameter governs the loss of water from actual evapotranspiration. Smaller the value of Srmax, lesser would be the amount of water available for evapotranspiration thereby resulting into increase in volume of the flow and higher the value of Srmax, greater would be the amount of water available for evapotranspiration resulting into decrease in volume of the flow. The Srmax was calculated for each grid cell using soil and land cover characteristics. However, user has to select one method in the settings window before calibration. The first method was using the option “calibrate”. Using this option, the values for Srmax were calibrated for 4 different types of reclassified land cover. The Srmax calibrated for Deep Rooted (DR), Shallow Rooted (Grass land) (SR), Shallow Rooted and Irrigated (SRI), and Impervious (IMP) were 0.022m, 0.018m, 0.012m and 0.0001m respectively.

The block average roughness coefficient (n_0) helps to adjust the overall shape of the hydrograph. The parameter n_0 is not very sensitive to volume however the higher value tends to reduce the volume of flow whereas the lower value tends to increase the volume of flow. The average value of n_0 in the Sunkoshi river basin was observed to be 0.164.

The drying function parameter (α) affects the actual evapotranspiration from the root zone. Therefore higher values of α increases loss of water reducing the volume of flow whereas lower value of α decreases loss of water increasing the volume of flow. The average value of drying function parameter in the Sunkoshi river basin was observed to be 0.013.

The saturation deficit (SD_{bar}) is another parameter representing soil property. Higher the value of SD_{bar}, lower would be the value of flow and vice-versa. The average value of SD_{bar} for the Sunkoshi basin was observed to be 0.01 m.

The two Muskingum-Cunge parameters, dt and dl, were used to sub-divide the time interval and the channel length for obtaining high accuracy. The optimized value of dt and dl were calibrated as 3.

7.3 PET Computation

The Shuttleworth-Wallace (S-W) model was used to calculate the potential evapotranspiration. The PET_o indicates potential evapotranspiration from the interception and PET indicates potential evapotranspiration from the root zone. The S-W model uses the publicly available dataset to calculate PET. The meteorological data were obtained from CRU data set.

The developed Shuttleworth-Wallace model is applicable particularly to the data poor or ungauged large basins. The table 7.2 and 7.3 shows PET computed by the Shuttleworth-Wallace model using global dataset for calibrated period, (i.e. from 1994 to 1997) and validation period (i.e. from 1998 to 2001) respectively.

Table 7.5

Avg. Monthly PET (mm) Computation in Calibration Period (1994 to 1997)

Months\Year	**1994**	**1995**	**1996**	**1997**
Jan	33.39	41.2	37.33	48.01
Feb	36.75	36.58	32.96	42.03
Mar	54.84	44.53	36.61	36.91
Apr	71.33	71.76	58.41	44.88
May	92.43	88.73	73.97	71.47
Jun	100.8	100.42	90.24	87.45
Jul	90.00	91.81	89.16	103.23
Aug	90.86	93.09	83.92	98.02
Sep	81.45	93.72	93.17	96.51
Oct	72.54	79.23	83.01	97.38
Nov	60.71	68.66	71.24	83.48
Dec	47.66	46.64	60.51	66.92
Total	**832.76**	**856.37**	**810.53**	**876.29**

Source: This Study

Fig 7.6

Avg. Monthly PET in Calibration Period (1994 to 1997)

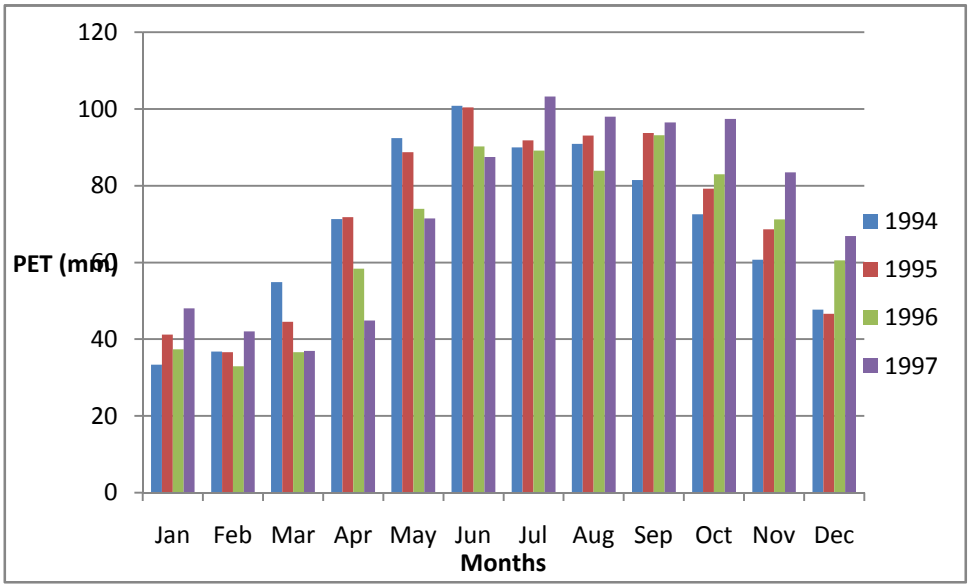

Fig 7.6

Avg. Monthly PET (mm) Computation in Validation Period (1998 to 2001)

Months\Year	1998	1999	2000	2001
Jan	32.65	41.9	37.29	44.4
Feb	35.74	36.97	32.83	40.46
Mar	56.74	45.85	36.65	36.1
Apr	76.13	73.46	52.71	43.5
May	89.71	85.7	66.24	66.8
Jun	98.55	97.71	76.34	75.22
Jul	89.27	100.28	86.33	92.88
Aug	79.53	87.88	86.79	88.9
Sep	77.53	81.46	77.67	88.41
Oct	69.94	74.23	77.74	87.62
Nov	61.19	69.26	70.81	72.85
Dec	48.3	46.48	57.54	68.38
Total	**815.28**	**841.18**	**758.94**	**805.52**

Source: This Study

Fig 7.7

Avg. Monthly PET in Validation Period (1998 to 2001)

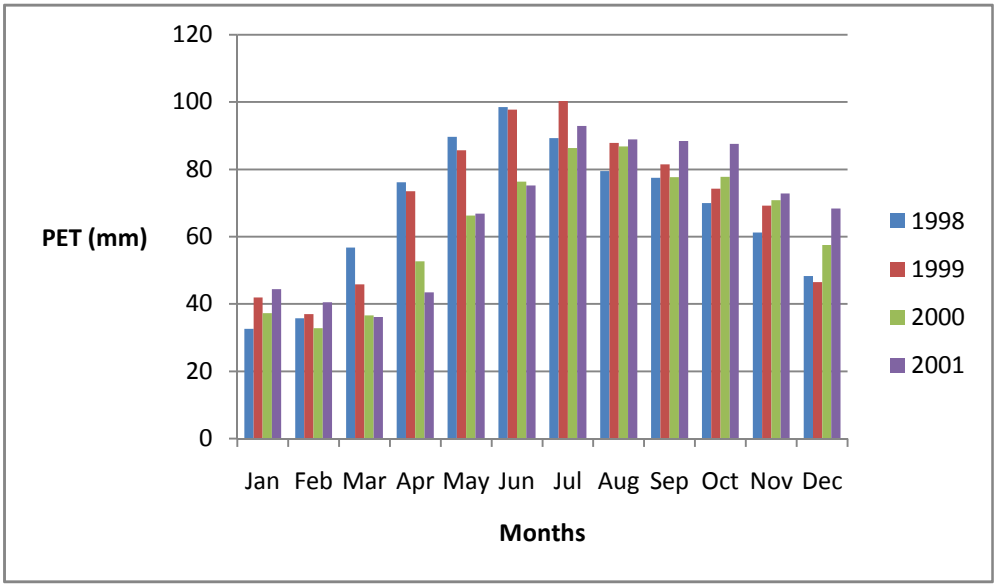

The monthly average of PET was computed using PET model of BTOPMC using monthly time series data of CRU TS 2.0 and monthly composite NOAA-AVHRR NDVI from 1994 to 2001. The Shuttleworth-Wallace model estimated the annual PET of 833 mm, 856 mm, 811 mm, 876 mm, 815 mm, 841 mm, 759 mm, and 806 mm in the year 1994, 1995, 1996, 1997, 1998, 1999, 2000, and 2001 respectively.

The model has also calculated the actual evapotranspiration (AP), potential evapotranspiration (EP), And, it is seen that when there is enough rainfall, actual evapotranspiration reaches nearly to its potential evapotranspiration.

The graph of actual evapotranspiration (EA) vs potential evapotranspiration (EP) is shown in figure 7.8.

Fig. 7.8

Actual Evapotranspiration (AP) Vs Potential Evapotranspiration (EP) (1994 – 1997)

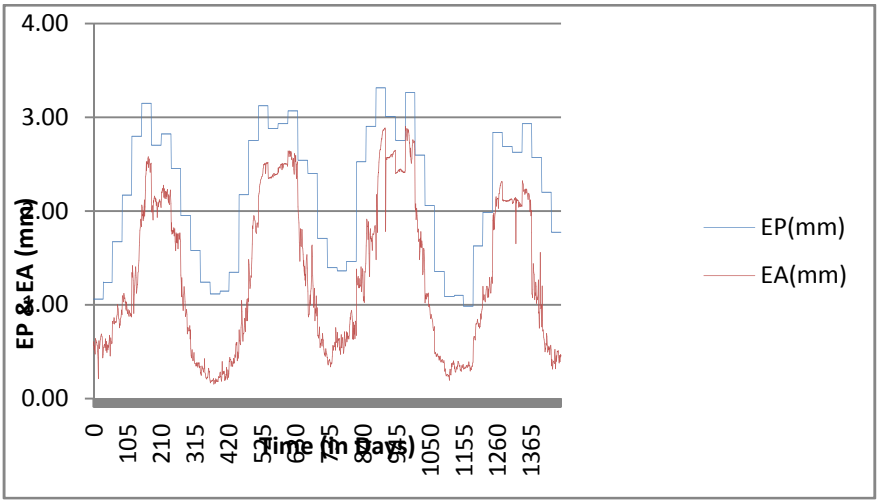

Fig 7.9

Actual Evapotranspiration (EA) Vs Potential Evapotranspiration (EP) (1998 – 2001)

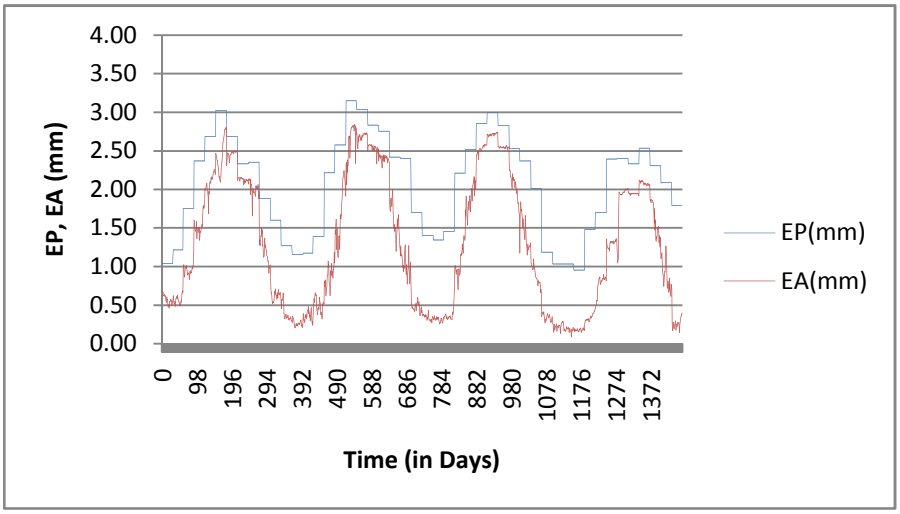

8. SUMMARY, CONCLUSION AND RECOMMENDATIONS

8.1 Summary

The BTOPMC refers to “Blockwise use of TOPMODEL with Muskingum-Cunge routing”. This model was developed at University of Yamanashi, Japan. It implements the concepts of TOPMODEL with Muskingum-Cunge method for flow routing. The model performs distributed calculations of flows, but it is conceptually semi-distributed in terms of parametrizations.

In Nepal, most of the river basins are data poor or ungauged so it may be the better option to use a runoff simulating tool that uses a global public domain datasets. Therefore, to calibrate and validate the model in the Sunkoshi river basin using local available hydrometeorological data and global public domain dataset was the main objective of the study.

The Sunkoshi river basin lies in the central northern part of the Nepal and is one of the river basins with good hydrology with a suitable topography for planning any type of hydropower projects. The total basin area of the Sunkoshi river basin at Pachhuwarghat gauging station is 4920 sq. km. It mainly covers two districts of Nepal (Sindhupalchok and Kavrepalanchok) and about 27 % of the total basin area lies in Tibet, China. The elevations in the basin under study range from 602 m, at gauging station in Pachhuwarghat, to 7786 m at high Himalaya. Owing to large differences in the elevations of the topography the basin is characterized by diversified climatic patterns. The study area receives an annual rainfall of 2300 mm.

The study covers eight years period from 1994 to 2001. The period of 1991 to 1997 was used for calibrating the model and the period of 1998 to 2001 was used for validating the same. The local available hydro meteorological data (discharge, rainfall, and temperature) were collected from DHM whereas other various global datasets were collected from different public domains. The model requires feed various kinds of data into its own standard format. To prepare data into the standard format, different tools like Arc view/Arc Info, MS Excel, Google Earth, Win BTOPMC preprocessor tool and other different tools provided by COE-UY were used. The processed data were finally fed into the model and results were analyzed to meet the objectives of the study.

8.2 Conclusions

The BTOPMC has been applied to the Sunkoshi River Basin and simulated the daily flows. The BTOPMC has an advantage of both lumped as well as distributed model. In BTOPMC, there are minimum number of parameters to be specified for each sub-basin which makes it more manageable.

From the results obtained from the model following conclusions can be drawn:

1. The Nash Sutcliffe Efficiency of 81.41 % with the volume ratio of 89.35 % and the volume bias of - 10.65 % was obtained in calibration of the model using the option “calculate using soil and land cover data” for Srmax computation. The Nash efficiency was very good and the VB was good.

2. The Nash Sutcliffe Efficiency of 82.87 % with the volume ratio of 101.05 % and volume bias of 1.05 % was obtained in validation of the model using the option “calculate using soil and land cover data” for Srmax computation. The Nash efficiency was very good and the VB was excellent.

3. The Nash Sutcliffe Efficiency of 81.67 % with the volume ratio of 99.67 % and volume bias of – 0.32 % was obtained in calibration of the model using the option “calibrate” for Srmax computation. The Nash efficiency was very good and the VB was excellent.

4. The Nash Sutcliffe Efficiency of 82.01 % with the volume ratio of 108.58 % and the volume bias of 8.59 % was obtained in validation of the model using the option “calibrate” for Srmax computation. The Nash efficiency as well as the VB were very good.

5. The Nash Sutcliffe Efficiency obtained by using the option “calculate using soil and land cover data” for Srmax computation was slightly better than that obtained from using the option “calibrate”.

6. The peak flows were underestimated which might be due to lack of sufficient number of rainfall stations in Sunkoshi River Basin.

7. The annual potential evapotranspiration values from the S-W model were estimated as 833 mm in 1994, 856 mm in 1995, 811 mm in 1996, 876 mm in 1997, 815 mm in 1998, 841 mm in 1999, 759 mm in 2000, and 806 mm in 2001.

8. The monthly snow cover area was computed in percentage of total basin area only for the year 1994 and was observed to be highest i.e., 47.78 % in February and lowest i.e., 18.09 % in August.

9. Finally, the BTOPMC is an applicable and reliable model for carrying out research in large river basins such as Sunkoshi River basin.

8.3 Recommendations

On the basis of analysis and findings of the study, following recommendations are made to improve the efficiency of the model.

1. The BTOPMC model can be used to estimate soil moisture content of the basin for further analysis such as soil classification and land cover parameters.
2. Meso-scale precipitation model, Sub-surface hydrological simulation models, sediment transport models, Inundation simulation model, Water quality model, water use/control model are in developing stage in BTOPMC. So, it can be used in solving different hydrological problems of different basins.
3. As the number of rain gauges is inadequate, sufficient number of rainfall measuring stations is required to be installed according to the norms laid down by WMO.
4. The BTOPMC model can also be used in climate change related studies of the large basins.

BIBLIOGRAPHIES

Aryal, Sagar (2007), **Application of a Distributed Hydrological Model-BTOPMC in Narayani River Basin**, An unpublished MSc Thesis, submitted to Pulchowk Campus, Institute of Engineering, TU

Bahadur, Jagadish (1993), **The Himalayas: A Third Polar Region**, Snow & Glaciers Hydrology, IAHS, Publ. No 218

Baral, Sanjeeb (2007), **Applicability of Semi-distributed Hydrological Model (BTOPMC) in Bagmati River Basin**, An unpublished MSc Thesis, submitted to Pulchowk Campus, Institute of Engineering, TU

Chow , V.T. et al (1998), **Applied Hydrology**, McGraw-Hill Publishers, New York

Dixit, Ajay (2002), **Basic Water Science**, 1st Edition, Kathmandu, Nepal Water Conservation Foundation

Dixit, Ajay (1995), **Resource Endowment and Associated Uncertainty of Water Resources**, Water Resources Development: Nepalese Perspective, Konark Publishers Pvt. Ltd, India.

Duggal, K. N. and Soni J.P. (1996), **Elements of Water Resources Engineering**, New Delhi, New Age International (P) Limited, Publishers

Dulal et al. (2006), **Evaluation of a Physically Based Distributed Hydrological Model, BTOPMC, for different physiographic zone of Nepal**.

Dulal, K. N. (2008), **BTOPMC Hydrological Model**, Kathmandu, CREEW

Garg, S. K. (2005), **Hydrology & Water Resources Engineering**, 13th Revised Edition, Delhi, Khanna Publishers

WMO (1994), **Guide to Hydrological Practices**, Fifth Edition, No. 168

Hapuarachchi et al. (2005**), Hydrological Modeling and Flood Simulation of the Fuji River Basin in Japan,** Proc. 7 th International River Symposium, Brisbane, Australia

Hapuarachchi et al. (2007), **Importance of Rainfall Measurements for the Flood Forecasting of the Mekong River Basin,** Proc. Of the Annual Mekong Flood Forum-5, Ho Chi Minh City, Vietnam.

Hapuarachchi et al. (2008), **Investigation of the Mekong River Basin Hydrology for 1980-2000 Using the YhyM**, Hydrological Processes, Wiley InterScience

Henriksen et al. (2003), **Methodology for Construction, Calibration and Validation of a National Hydrological Model for Denmark**, Journal of Hydrology, Vol. 280, pp. 52 – 71.

Ishidaira et al. (2006), **Relating to BTOPMC Model Parameters to Physical Features of MOPEX Basins**, Journal of Hydrology, Vol. 320, pp. 84 – 102.

Kayastha et al. (2000), **Positive Degree – Day factors for Ablation on Glaciers in the Nepalese Himalayas: Case Study on Glacier AX010 in Shorong Himal**, Nepal.

Kayastha et al. (2003), **Positive Degree – Day Factors for Ice Ablation on Four Glaciers in the Nepalese Himalayas and Qinghai – Tibetan Plateau**, Japanese Society of Snow and Ice, Japan.

Kayastha, Rijan B. (2009), **Estimation of Discharge from Glacerized Basins of Nepal and Possible Impact of Climate Change on Discharge in the Langtang Valley, Nepal,** Proc. Of the TWAS Young Scientists of Asia Conclave on Pressing Problems of Humankind-Energy and Climate, Banglore, India, pp. 78 – 85.

Khanal, Narendra; Shrestha, Mandira and Ghimire, Motilal (2007), **Preparing for Flood Disaster: Mapping and Assessing Hazard in the Ratu Watershed, Nepal**, Kathmandu, ICIMOD

Ranjit (2002), **The Current Status of Capture Fishery in the Upper Sunkoshi River**, Cold Water Fisheries in the Trans-Himalayan Countries, FAO, Vol. 431, Rome

Reddy, Jaya Ram (2006), **A Textbook of Hydrology**, 2nd Edition, New Delhi, Laxmi Publications (P) Ltd

Shilpakar et al. (2009), **Impact of Climate Change on Snowmelt Runoff: A Case Study of Tamakoshi Basin in Nepal**

Shrestha et al. (2007), **The Assessment of Spatial and Temporal Transferability of a Physically Based Distributed Hydrological Model Parameters in Different Physiographic Regions of Nepal**, Journal of Hydrology, Vol. 347, pp. 153-172

Suresh, R. (1997), **Watershed Hydrology**, 1st Edition, Delhi, Standard Publishers Distributors

Takeuchi et al. (2007), **A BTOP Model to Extend TOPMODEL for Distributed Hydrological Simulation of Large Basins**, Hydrological Processes, Wiley InterScience.

Takeuchi, Kuniyoshi et al. (1999), **Introduction of Block-wise Use of TOPMODEL and Muskingum-Cunge Method for the Hydro-Environmental Simulation of a Large Ungauged Basin**, Hydrological Sciences Journal, Vol. 44, No 4, pp. 633-645

Thapa and Pradhan (1995), **Water Resources Development**, New Delhi, Konark Publishers Pvt. Ltd.

US Army Corps of Engineers (2001), **Hydrologic Modeling System HEC-HMS**, User's Manual, Davis, California

Varshney, R. S. (1986), **Engineering Hydrology**, 3rd Edition, Roorkee, Nem Chand & Bros

Verghese and Iyer (1994), **Harnessing the Eastern Himalayan Rivers,** 2nd Impression**,** New Delhi, Konark Publishers Pvt. Ltd.

Zhou et al. (2006), **Estimating Potential Evapotranspiration Using Shuttleworth-Wallace Model and NOAA-AVHRR NDVI Data to Feed a Distributed Hydrological Model Over the Mekong River Basin**, Journal of Hydrology, Vol. 327, No. 1 -2, pp. 151 – 173

Websites:

http://erg.com.np/hydropower_national.php

http://water.oregonstate.edu/streamflow/analysis/annual/index.htm

http://www.dhm.gov.np

http://www.terraseer.com/data/spacestat_nepal.php

http://hydro.iis.u-tokyo.ac.jp/GAME-T/GAIN-T/routine/nepal/index.html

Appendix No 1

Sample of DEM data

ncols 92
nrows 98
xllcorner 85.45
yllcorner 27.55
cellsize 0.008333
NODATA_value -9999
3004 3391 3760 4162 4423 4618 4036 3735 3684 3931 4426 5008 5350 5412 5418 5529 5420 5046 4786
4796 5287 5525 5312 5458 5726 5687 5743 5741 5615 5379 5444 5680 6108 6058 6004 6423 6841 7127
7321 7428 7272 7179 7190 7087 6514 5814 5593 5379 5324 5293 5256 5214 5214 5229 5157 5121 5153
5123 5041 4941 4809 4712 4669 4689 4710 4730 4838 4753 4509 4428 4510 4493 4279 4252 4272 4302
4358 4397 4589 4736 4731 4564 4700 4830 4925 4993 5066 5355 5530 5581 5659 5451
3012 3371 3923 4302 4359 4097 3617 3490 3879 4142 4588 5012 5264 5568 5378 5166 5070 4710 4635
5016 5272 5546 5533 5865 6108 6242 5749 5606 5443 5319 5336 5624 5947 5956 5886 5903 6121 6667
7308 7786 7582 7251 7208 7102 6533 5712 5834 5585 5671 5593 5377 5258 5258 5244 5213 5250 5211
5216 5154 5072 4944 4837 4769 4792 4908 4963 5086 5152 4918 4795 4887 4638 4260 4279 4526 4603
4722 4422 4520 4686 4553 4660 4845 5021 5218 5255 5238 5321 5493 5708 5764 5626
2891 3186 3611 3673 3718 3568 3317 3710 4295 4603 5125 5542 5832 5867 5480 4943 4533 4590 4940
5175 5444 5660 5904 5717 5736 6110 5785 5626 5631 5252 5265 5519 5756 5931 5818 5808 5888 5939
6449 7065 7435 6737 6095 6023 5919 5391 5298 5322 5412 5516 5348 5222 5293 5472 5349 5363 5240
5322 5223 5093 5045 5025 5004 4895 5082 5152 5179 5190 5071 5009 4773 4393 4220 4537 4797 4952
4899 4643 4487 4517 4605 4786 5002 5201 5378 5509 5559 5496 5446 5706 5890 5780
2696 2781 2848 2949 3086 3140 3218 3513 3770 4161 4625 5158 5541 5349 5049 4496 4495 5068 5381
5505 5835 5865 5692 5470 5505 5939 5625 5489 5350 5160 5302 5459 5772 5948 5770 5740 5713 5751
5866 6277 6888 7190 6230 5853 5474 5237 5148 5230 5243 5290 5178 5179 5405 5546 5475 5345 5335
5355 5193 5345 5370 5288 5051 5010 5249 5302 5236 4933 4774 4757 4551 4211 4276 4579 4850 5014
4993 4988 4902 4800 4793 4986 5261 5478 5557 5768 5908 5741 5505 5514 5827 5940
2904 3170 3176 3232 3073 3341 3710 3543 3583 3714 4288 4656 5028 4940 4556 4338 4802 5180 5430
5649 5941 5672 5414 5352 5652 5962 5637 5382 5200 5086 5403 5859 6224 6300 5843 5699 5655 5733
5863 5994 6546 6827 6234 5707 5290 5143 5119 5129 5202 5170 5164 5230 5516 5707 5469 5413 5489
5312 5355 5617 5441 5199 5039 5119 5270 5130 4977 4879 4581 4399 4214 4206 4418 4625 4729 4745
4787 4846 4911 5019 5031 5101 5272 5410 5552 5764 6045 5984 5788 5543 5645 5726
3107 3374 3796 3673 3241 3388 4019 4342 4087 3885 3892 4006 4427 4281 4336 4635 4809 4974 5136
5505 5758 5395 5315 5292 5819 5742 5521 5227 5101 5020 5021 5417 5402 5710 6035 5630 5609 5720
5701 5746 6204 6528 6030 5824 5703 5334 5103 5100 5195 5203 5276 5243 5475 5685 5489 5609 5491
5353 5394 5390 5226 5121 5107 5213 5123 4977 4748 4722 4588 4282 4166 4308

Appendix No 2

Sample of Land Cover Data

ncols 92
nrows 98
xllcorner 85.4500000000
yllcorner 27.5500000000
cellsize 0.0083333333
nodata_value -9999.0000000000
14 14 4 4 10 10 10 10 10 10 7 7 7 7 7 7 7 7 7 7 7 16 16 16 16 15 15 15 15 15 15 15
15 15 15 15 15 15 15 15 15 15 15 15 15 15 15 15 16 16 16 16 16 7 7 7 7 7 7 7 7 7 7 7 7
7 7 7 7 7 7 7 7 7 7 7 7 7 7 7 7 7 7 7 7 7 7 7 7 7 7 7 7
14 14 12 10 10 10 1 4 10 7 7 7 7 7 7 7 7 7 7 7 16 16 16 16 15 15 15 15 15 15 15 15
15 15 15 15 15 15 15 15 15 15 15 15 15 15 15 16 16 16 16 16 16 16 16 16 7 7 7 7 7 7 7 7 7
7 7 7 7 7 7 7 7 7 7 7 7 7 7 7 7 7 7 7 7 7 7 7 7 7 7 7 16 7
14 12 12 1 1 1 1 1 10 10 7 7 7 7 7 7 7 7 7 7 7 16 16 16 15 15 15 15 15 15 15 15 15
15 15 15 15 15 15 15 15 15 15 15 15 16 16 16 16 16 16 16 16 7 7 7 7 7 7 7 7 7 7 7 7 7
7 7 7 7 7 7 7 7 7 7 7 7 7 7 7 7 7 7 7 7 7 7 7 7 16 16 7 16 16
10 14 1 14 14 1 1 10 10 10 10 7 7 7 7 7 7 7 7 16 16 16 16 15 15 15 15 15 15 15 15 15
15 15 15 15 15 15 15 15 15 15 15 15 16 16 16 16 16 16 16 16 16 16 7 7 7 7 7 7 7 7 7 7
7 7 7 7 7 7 7 7 7 7 7 7 7 7 7 7 7 7 7 7 7 7 7 7 16 16 16 16 16 16
14 14 1 1 1 1 1 10 12 10 10 10 10 7 7 7 10 10 7 7 16 16 16 16 16 15 15 15 15 15 15 15
15 15 16 15 15 15 15 15 15 15 15 15 15 15 16 16 17 17 17 16 16 16 16 16 7 7 7 7 7 7 7 7
7 7 7 7 7 7 7 7 7 7 7 7 7 7 7 7 7 7 7 7 7 7 7 7 16 16 16 16 16 16 16 16
1 1 1 1 10 10 10 10 7 7 7 10 7 7 7 10 7 7 7 7 16 16 16 16 15 15 15 15 15 16 16 16 15
16 15 15 15 15 15 15 15 15 15 15 15 15 16 16 16 16 16 16 16 16 16 7 7 16 16 16 7 7 7 7 7 7
7 7 7 7 7 7 7 7 7 7 7 7 7 7 7 7 7 7 7 7 7 16 16 16 16 16 16 16 16 16
1 10 10 10 10 10 10 10 10 7 7 7 7 7 7 7 7 7 16 16 16 16 16 15 15 15 15 15 15 16 15 15
15 15 15 15 15 16 16 16 16 16 15 15 15 15 16 16 16 16 16 16 7 16 16 16 16 16 16 7 7 7 7 7 7
7 7 7 7 7 7 7 7 7 7 7 7 7 7 7 7 7 7 7 7 7 7 7 7 16 16 16 16 16 16 16 16

Appendix No 3

Sample of Soil Data

ncols 92
nrows 98
xllcorner 85.45
yllcorner 27.55
cellsize 0.008333
NODATA_value -9999
3717 3717 3717 3717 3717 3717 3717 3717 3717 3717 3717 3717 3717 6998 6998 6998 6998 6998 6998
6998 3717 3717 3717 3717 3717 3717 3717 3717 3717 3717 3717 3717 6998 6998 6998 6998 6998 6998
6998 6998 6998 6998 6998 6998 6998 6998 6998 6998 6998 6998 6998 3717 3717 3717 3717 3717 3717
3717 3717 3717 3717 3717 3717 3717 3717 3717 3717 3717 3717 3717 3717 3717 3717 3717 3717 3717
3717 3717 3717 3717 3717 3717 3717 3717 3717 3717 3717 3717 3717 3717 3717
3717 3717 3717 3717 3717 3717 3717 3717 3717 3717 3717 3717 3717 6998 6998 6998 6998 6998 6998
6998 3717 3717 3717 3717 3717 3717 3717 3717 3717 3717 3717 3717 3717 6998 6998 6998 6998 6998
6998 6998 6998 6998 6998 6998 6998 6998 6998 6998 6998 6998 6998 3717 3717 3717 3717 3717 3717
3717 3717 3717 3717 3717 3717 3717 3717 3717 3717 3717 3717 3717 3717 3717 3717 3717 3717 3717
3717 3717 3717 3717 3717 3717 3717 3717 3717 3717 3717 3717 3717 3717 3717
3717 3717 3717 3717 3717 3717 3717 3717 3717 3717 3717 3717 3717 6998 6998 6998 6998 6998
6998 3717 3717 3717 3717 3717 3717 3717 3717 3717 3717 3717 3717 3717 6998 6998 6998 6998
6998 6998 6998 6998 6998 6998 6998 6998 6998 6998 6998 6998 6998 3717 3717 3717 3717 3717 3717
3717 3717 3717 3717 3717 3717 3717 3717 3717 3717 3717 3717 3717 3717 3717 3717 3717 3717 3717
3717 3717 3717 3717 3717 3717 3717 3717 3717 3717 3717 3717 3717 3717 3717
3717 3717 3717 3717 3717 3717 3717 3717 3717 3717 3717 3717 3717 6998 6998 6998 6998 6998
3717 3717 3717 3717 3717 3717 3717 3717 3717 3717 3717 3717 3717 3717 3717 6998 6998 6998 6998
6998 6998 6998 6998 6998 6998 6998 6998 6998 6998 6998 6998 6998 3717 3717 3717 3717 3717 3717
3717 3717 3717 3717 3717 3717 3717 3717 3717 3717 3717 3717 3717 3717 3717 3717 3717 3717 3717
3717 3717 3717 3717 3717 3717 3717 3717 3717 3717 3717 3717 3717 3717 3717
3717 3717 3717 3717 3717 3717 3717 3717 3717 3717 3717 3717 3717 6998 6998 6998 6998 6998
3717 3717 3717 3717 3717 3717 3717 3717 3717 3717 3717 3717 3717 3717 3717 6998 6998 6998
6998 6998 6998 6998 6998 6998 6998 6998 6998 6998 6998 6998 6998 3717 3717 3717 3717 3717 3717
3717 3717 3717 3717 3717 3717 3717 3717 3717 3717 3717 3717 3717 3717 3717 3717 3717 3717 3717
3717 3717 3717 3717 3717 3717 3717 3717 3717 3717 3717 3717 3717 3717 3717
3717 3717 3717 3717 3717 3717 3717 3717 3717 3717 3717 3717 3717 6998 6998 6998 6998 6998
3717 3717 3717 3717 3717 3717 3717 3717 3717 3717 3717 3717 3717 3717 3717 3717 3717 3717 3717
3717 3717 3717 3717 3717 3717 3717 3717 3717 3717 3717 3717 3717 3717 3717 3717 3717 3717 3717
3717 3717 3717 3717 3717 3717 3717 3717 3717 3717 3717 3717 3717 3717 3717 3717 3717 3717 3717
3717 3717 3717 3717 3717 3717 3717 3717 3717 3717 3717 3717 3717 3717 3717

Appendix No 4

Sample of Discharge Data

1	0
1994010100	27.558
2001123100	85.752
1994010100	49.4
1994010200	49.4
1994010300	48.6
1994010400	48.6
1994010500	47.8
1994010600	47.8
1994010700	47.8
1994010800	47
1994010900	47
1994011000	47
1994011100	47
1994011200	46.2
1994011300	46.2
1994011400	45.4
1994011500	46.2
1994011600	50.2
1994011700	51
1994011800	48.6
1994011900	47.8
1994012000	46.2
1994012100	45.4
1994012200	45.4
1994012300	44.6
1994012400	45.4
1994012500	44.6
1994012600	45.4
1994012700	46.2
1994012800	47.8
1994012900	47
1994013000	46.2
1994013100	45.4
1994020100	45.4
1994020200	44.6
1994020300	47
1994020400	46.2
1994020500	46.2
1994020600	45.4
1994020700	44.6
1994020800	40.6

Appendix No 5

Sample of Rainfall Data

12	0	1	2	3	4	5	6	7	8	9	10	11	
1994010100		27.866	27.8	27.783	27.783	27.7	27.633	27.916	27.783	27.683	28	27.7	27.7
2001123100		85.866	85.61	85.716	85.566	85.65	85.716	85.633	85.9	85.633	85.55	85.716	85.7
1994010100		0	0	0	0	0	0	0	0	0	0	0	0
1994010200		0	0	0	0	0	0	0	0	0	0	0	0
1994010300		0	0	0	0	0	0	0	0	0	0	0	0
1994010400		0	0	0	0	0	0	0	0	0	0	0	0
1994010500		0	0	0	0	2.5	0	0	0	0	0	0	0
1994010600		0	0	0	0	0	0	0	0	0	0	0	0
1994010700		0	0	0	0	0	0	0	0	0	0	0	0
1994010800		0	0	0	0	0	0	0	0	0	0	0	0
1994010900		0	0	0	0	0	0	0	0	0	0	0	0
1994011000		0	0	0	0	0	0	0	0	0	0	0	0
1994011100		0	0	0	0	0	0	0	0	0	0	0	0
1994011200		0	0	0	0	0	0.3	0	0	0	0	0	0
1994011300		0	0.1	0	0	0	0	0	0	0	0	0	0
1994011400		0	0	0	0	0	0	0	0	0	0	0	0
1994011500		0	0	0	24.3	10.5	0	0	10	0	0	0	0
1994011600		10.5	20	0	10.2	17.1	14.5	0	0	13.9	12.5	0	18
1994011700		10	20.8	0	4.1	0	7.2	0	35.5	0	16.2	23.2	12
1994011800		5	0	0	0	0	0	0	0	0	0	0	17
1994011900		0	0	0	0	0	0	0	0	0	0	0	0
1994012000		0	0	0	0	0	0	0	0	0	0	0	0
1994012100		0	0	0	0	0	0	0	0	0	0	0	0
1994012200		0	0	0	0	0	0	0	0	0	0	0	0
1994012300		0	0	0	0	0	0	0	0	0	0	0	0
1994012400		0	0	0	0	0	0	0	0	0	0	0	0
1994012500		0	0	0	0	0	0	0	0	0	0	0	0
1994012600		0	0	0	0	0	0	0	0	0	0	0	0
1994012700		0	0	0	0	0	0	0	0	0	0	0	0
1994012800		0	0	0	0	0	0	0	0	0	0	0	0
1994012900		0	0	0	0	0	0	0	0	0	0	0	0
1994013000		0	0.1	0	0	0	0	0	0	0	0.4	0	0
1994013100		0	0	0	0	0	0	0	0	0	0	0	0
1994020100		0	1.6	0	2.1	1.5	0	0	0	0	1.8	0	0
1994020200		0	0	0	0	0	2.3	0	2	0	6	0	1
1994020300		0	0	0	0	0	0	0	0	0	0	0	0
1994020400		0	0	0	0	0	0	0	0	0	2.4	0	0
1994020500		0	0	0	0	0	0	0	0	0	0	0	0
1994020600		0	0	0	0	0	0	0	0	0	0	0	0
1994020700		0	0	0	0	0	0	0	0	0	0	0	0
1994020800		0	0	0	0	0	0	0	0	0	0	0	0

Appendix No 6

Sample of Temperature Data

1	0
1994010100	27.9791
2001123100	85.8881
1994010100	-6.0
1994010200	-4.0
1994010300	-7.3
1994010400	-5.5
1994010500	-7.5
1994010600	-8.5
1994010700	-1.3
1994010800	-2.0
1994010900	-2.3
1994011000	-3.3
1994011100	-2.6
1994011200	-4.0
1994011300	-4.3
1994011400	-6.5
1994011500	-9.3
1994011600	-14.3
1994011700	-7.0
1994011800	-4.0
1994011900	-6.8
1994012000	-7.3
1994012100	-5.3
1994012200	-3.0
1994012300	-2.5
1994012400	-0.3
1994012500	1.8
1994012600	2.3
1994012700	0.5
1994012800	0.3
1994012900	-5.0
1994013000	-9.3
1994013100	-8.0
1994020100	-8.3
1994020200	-8.3
1994020300	-7.5
1994020400	-7.0
1994020500	-7.0
1994020600	-7.8
1994020700	-4.3
1994020800	-6.8

Appendix No 7

Sample of a Control File

#Name_of_the_file	Num
D:\sunkoshi_river\ndvi\ndvi_94_jan.asc	31
D:\sunkoshi_river\ndvi\ndvi_94_feb.asc	28
D:\sunkoshi_river\ndvi\ndvi_94_mar.asc	31
D:\sunkoshi_river\ndvi\ndvi_94_apr.asc	30
D:\sunkoshi_river\ndvi\ndvi_94_may.asc	31
D:\sunkoshi_river\ndvi\ndvi_94_jun.asc	30
D:\sunkoshi_river\ndvi\ndvi_94_jul.asc	31
D:\sunkoshi_river\ndvi\ndvi_94_aug.asc	31
D:\sunkoshi_river\ndvi\ndvi_94_sep.asc	30
D:\sunkoshi_river\ndvi\ndvi_94_oct.asc	31
D:\sunkoshi_river\ndvi\ndvi_94_nov.asc	30
D:\sunkoshi_river\ndvi\ndvi_94_dec.asc	31
D:\sunkoshi_river\ndvi\ndvi_95_jan.asc	31
D:\sunkoshi_river\ndvi\ndvi_95_feb.asc	28
D:\sunkoshi_river\ndvi\ndvi_95_mar.asc	31
D:\sunkoshi_river\ndvi\ndvi_95_apr.asc	30
D:\sunkoshi_river\ndvi\ndvi_95_may.asc	31
D:\sunkoshi_river\ndvi\ndvi_95_jun.asc	30
D:\sunkoshi_river\ndvi\ndvi_95_jul.asc	31
D:\sunkoshi_river\ndvi\ndvi_95_aug.asc	31
D:\sunkoshi_river\ndvi\ndvi_95_sep.asc	30
D:\sunkoshi_river\ndvi\ndvi_95_oct.asc	31
D:\sunkoshi_river\ndvi\ndvi_95_nov.asc	30
D:\sunkoshi_river\ndvi\ndvi_95_dec.asc	31
D:\sunkoshi_river\ndvi\ndvi_96_jan.asc	31
D:\sunkoshi_river\ndvi\ndvi_96_feb.asc	29
D:\sunkoshi_river\ndvi\ndvi_96_mar.asc	31
D:\sunkoshi_river\ndvi\ndvi_96_apr.asc	30
D:\sunkoshi_river\ndvi\ndvi_96_may.asc	31
D:\sunkoshi_river\ndvi\ndvi_96_jun.asc	30
D:\sunkoshi_river\ndvi\ndvi_96_jul.asc	31
D:\sunkoshi_river\ndvi\ndvi_96_aug.asc	31
D:\sunkoshi_river\ndvi\ndvi_96_sep.asc	30
D:\sunkoshi_river\ndvi\ndvi_96_oct.asc	31
D:\sunkoshi_river\ndvi\ndvi_96_nov.asc	30
D:\sunkoshi_river\ndvi\ndvi_96_dec.asc	31
D:\sunkoshi_river\ndvi\ndvi_97_jan.asc	31
D:\sunkoshi_river\ndvi\ndvi_97_feb.asc	28
D:\sunkoshi_river\ndvi\ndvi_97_mar.asc	31
D:\sunkoshi_river\ndvi\ndvi_97_apr.asc	30
D:\sunkoshi_river\ndvi\ndvi_97_may.asc	31

Appendix No 8

Sub-basin Division

Basin ID	Longitude (X)	Latitude (Y)
0	85.972	27.979
1	85.820	27.752
2	85.778	27.743
3	85.576	27.777
4	85.736	27.558

Appendix No 9

Field Capacity (FC) and Permanent wilting point (WP) for USDA soil classification

Type	FC	WP
Sand	0.15	0.02
Loamy sand	0.125	0.035
Sandy loam	0.207	0.041
Loam	0.27	0.027
Silt loam	0.33	0.015
Sandy clay loam	0.255	0.068
Clay loam	0.318	0.075
Silty clay loam	0.366	0.04
Sandy clay	0.339	0.109
Silty clay	0.387	0.056
Clay	0.396	0.09
Silt	0.32	0.05

Appendix No 10

Root Depth for Different land Cover Types

ID	Land cover	Root depth (m)
1	Evergreen needle leaf forest	2.5
2	Evergreen broad leaf forest	2.5
3	Deciduous needle leaf forest	2.5
4	Deciduous broad leaf forest	2.5
5	Mixed forest	2.0
6	Closed shrublands	1.0
7	Open shrublands	1.0
8	Woody savannas	1.0
9	Savannas	1.0
10	Grasslands	0.5
11	Permanent wetlands	1.0
12	Croplands	0.7
13	Urban and built up	0.001
14	Cropland/Natural vegetation mosaic	1.0
15	Snow and ice	1.0
16	Barren or sparsely vegetated	1.0
17	Water bodies	0.001